© 2014. Published by The Company of Biologists Ltd | Journal of Cell Science (2014) 127, 5273–5287 doi:10.1242/jcs.157024

RESEARCH ARTICLE

DAPK–HSF1 interaction as a positive-feedback mechanism stimulating TNF-induced apoptosis in colorectal cancer cells

Natalya Benderska[1], Jelena Ivanovska[1], Tilman T. Rau[1], Jan Schulze-Luehrmann[1], Suma Mohan[2], Saritha Chakilam[1], Muktheshwar Gandesiri[1], Elisabeth Ziesché[3], Thomas Fischer[4], Stephan Söder[1], Abbas Agaimy[1], Luitpold Distel[5], Heinrich Sticht[6], Vijayalakshmi Mahadevan[2] and Regine Schneider-Stock[1,*]

ABSTRACT

Death-associated protein kinase (DAPK) is a serine-threonine kinase with tumor suppressor function. Previously, we demonstrated that tumor necrosis factor (TNF) induced DAPK-mediated apoptosis in colorectal cancer. However, the protein–protein interaction network associated with TNF–DAPK signaling still remains unclear. We identified HSF1 as a new DAPK phosphorylation target in response to low concentrations of TNF and verified a physical interaction between DAPK and HSF1 both *in vitro* and *in vivo*. We show that HSF1 binds to the DAPK promoter. Transient overexpression of HSF1 protein led to an increase in DAPK mRNA level and consequently to an increase in the amount of apoptosis. By contrast, treatment with a DAPK-specific inhibitor as well as DAPK knockdown abolished the phosphorylation of HSF1 at Ser230 ($pHSF1^{Ser230}$). Furthermore, translational studies demonstrated a positive correlation between DAPK and $pHSF1^{Ser230}$ protein expression in human colorectal carcinoma tissues. Taken together, our data define a novel link between DAPK and HSF1 and highlight a positive-feedback loop in DAPK regulation under mild inflammatory stress conditions in colorectal tumors. For the first time, we show that under TNF the pro-survival HSF1 protein can be redirected to a pro-apoptotic program.

KEY WORDS: DAPK, HSF1, TNF, Apoptosis, Colon, Cancer

INTRODUCTION

Death-associated protein kinase (DAPK) is a serine/threonine protein kinase that has been originally characterized as a tumor suppressor (Bialik and Kimchi, 2006; Bovellan et al., 2010; Michie et al., 2010; Raval et al., 2007) owing to its predominant function in the promotion of cell death (Eisenberg-Lerner and Kimchi, 2007; Jin and Gallagher, 2003; Raveh et al., 2001; Zalckvar et al., 2009). Hypermethylation of the DAPK promoter, which leads to the loss of protein expression, was found in different types of tumors (Benderska and Schneider-Stock, 2014; Kissil et al., 1997; Leung et al., 2008) and was shown to be associated with tumor progression and metastasis (Raveh and Kimchi, 2001).

DAPK is upregulated in response to various cytokines such as interferon γ (Deiss et al., 1995), transforming growth factor β (Jang et al., 2002), Fas and tumor necrosis factor α (TNF) (Cohen et al., 1999; Rennier and Ji, 2012). TNF plays a dual role in activating both pro- and anti-apoptotic mechanisms (Holtmann et al., 1988). In the gut, TNF induces DAPK-mediated apoptosis in tumor cells, whereas normal intestinal epithelial cells seem to be resistant to TNF but show remarkable DAPK-dependent inflammation (Bajbouj et al., 2009; Benderska et al., 2012; Chakilam et al., 2013). This suggests a cell-type-specific DAPK-mediated response to different stimuli (Schneider-Stock, 2014). Multi-domain structural organization of DAPK, which includes the catalytic domain, a Ca^{2+}/calmodulin-binding region, eight ankyrin repeats, two putative nucleotide-binding domains (P-loops), a cytoskeleton/Ras of complex proteins (ROC) domain and the C-terminal death domain, is responsible not only for direct protein phosphorylation of its substrates (Bialik and Kimchi, 2012; Kuo et al., 2003) but also for stabilization of multi-protein complexes in the cell (Ivanovska et al., 2013).

So far, little is known about the DAPK interactome in response to TNF. To gain further understanding of the role and function of the DAPK interaction network in tumor cells under inflammatory conditions, we performed a phosphopeptide array analysis. We identified heat-shock transcription factor 1 (HSF1) as a new candidate for DAPK phosphorylation under TNF stress. Under native conditions, human HSF1 exists in the cytoplasm in a monomeric form in which DNA-binding and transcriptional activity is repressed (Wu, 1995). In response to heat shock or other extracellular signals, HSF1 undergoes trimerization and translocates to the nucleus, where it specifically binds to the heat-shock response elements (HSE) in the promoter regions of target genes and induces their transcription (Morimoto, 1998; Wu, 1995). Phosphorylation on multiple serine and threonine residues is an important regulatory mechanism of HSF1 activation. The Ser230 is one of three currently known phosphorylation sites (along with Ser326, Ser320) associated with stimulation of transcription by HSF1 (Calderwood et al., 2010; Holmberg et al., 2001; Murshid et al., 2010). Nuclear translocation as well as HSF1 trimerization is not dependent on HSF1 Ser230 phosphorylation.

The major role of the evolutionarily highly conserved HSF1 is to protect cells from cell death by amplifying heat shock proteins (HSPs) that assist protein folding and prevent protein degradation. Otherwise, HSF1 promotes apoptotic cell death in male germ cells (Nakai et al., 2000) and sensitizes HeLa cells

[1]Department of Experimental Tumor Pathology, Institute of Pathology, Friedrich-Alexander University Erlangen-Nürnberg (FAU), Erlangen 91054, Germany. [2]Faculty of School of Chemical & Biotechnology of the SASTRA University, Thanjavur 613401, India. [3]3rd Medical Department, Medical University, 55122 Mainz, Germany. [4]Center of Internal Medicine, Clinic of Hematology/Oncology, Otto-von-Guericke University Magdeburg, 39106 Magdeburg, Germany. [5]Department of Radiation Oncology, University Erlangen-Nürnberg, 91054 Erlangen, Germany. [6]Institute of Biochemistry, Friedrich-Alexander University Erlangen-Nürnberg (FAU), Erlangen 91054, Germany.

*Author for correspondence (regine.schneider-stock@uk-erlangen.de)

Received 22 May 2014; Accepted 20 October 2014

Journal of Cell Science

to Fas-mediated killing (Xia et al., 2000), demonstrating antagonistic duality. In a mouse model, loss of HSF1 function contributes to genomic instability and the attenuation of adaptive reaction to intra- and extracellular signals (Mendillo et al., 2012; Min et al., 2007). Besides its significance in the heat shock program, HSF1 protein is overexpressed in many tumor types and is involved in tumor transformation (Mendillo et al., 2012).

Our study deciphers and functionally characterizes a new protein interaction complex between pro-apoptotic DAPK and pro-survival transcription factor HSF1 that mediates a TNF-induced pro-apoptotic cell response. To our knowledge, it is the first report indicating pro-apoptotic properties of HSF1 in tumor cells under inflammatory conditions. We show that direct HSF1 phosphorylation on Ser230 by DAPK plays an essential role in the formation of a positive-feedback loop to increase DAPK protein levels under conditions of mild cellular pro-inflammatory stress.

RESULTS

pHSF1^{Ser230} level is upregulated in colorectal cancer owing to TNF signaling

To identify new DAPK targets under conditions of TNF stress, we performed a phosphopeptide microarray analysis. We selected peptide sequences using two main criteria: (1) the exclusion of tyrosine phosphorylation and (2) the use of peptides containing the DAPK-specific phosphorylation consensus motif K/RXXS/T and an expanded sequence KRRXXS/T (where X is a random amino acid) (Bialik et al., 2008; Pike et al., 2008). As a result, we found 17 potential DAPK targets (supplementary material Table S1). Among them, HSF1 phosphorylation on Ser230 (referred to here as pHSF1^{Ser230}) led to a 1.85-fold increase in pHSF1^{Ser230} in response to TNF. Peptide alignment of HSF1 from different species identified Ser230 as an evolutionarily conserved site (Fig. 1A). Phosphopeptide array data were verified by western blotting (Fig. 1B) showing an increase in DAPK and pHSF1^{Ser230} protein levels over time in response to TNF. After knockdown of DAPK with short hairpin (sh)RNA, HSF1 phosphorylation at Ser230 was abolished (Fig. 1B). Next, we tested the expression of phosphorylated HSF1 in human colorectal carcinoma tissues. Indeed, the expression level of pHSF1^{Ser230} in lesions was greater than in investigated colorectal cancer cell lines (Fig. 1C).

It was shown that Ca^{2+}/calmodulin-dependent protein kinase (CaMKII) can also phosphorylate HSF1 at Ser230 (Holmberg et al., 2001). To investigate how DAPK and CaMKII interact with HSF1 individually, a model of the DAPK–pHSF1^{Ser230}–CAMKII complex was generated by computational docking, and this model revealed that DAPK and CAMKII have the same binding region in HSF1 (Fig. 1D). The interactions between HSF1–CAMKII and HSF1–DAPK are depicted in supplementary material Tables S2 and S3. There are several residues of HSF1 that participate in interactions between DAPK and CAMKII: Ser221, Tyr225, Arg227, Gln228, Ser230, His233, Ser237, Tyr240 and Pro245. Because these residues are involved in the consensus phosphorylation motif of HSF1 around Ser230, there might be competitive binding to HSF1. Using DAPK-specific and CAMKII-specific (KN62) inhibitors, we showed that the combination of TNF and DAPK inhibitor eliminated the phosphorylation of HSF1^{S230}, whereas KN62 did not change the levels of pHSF^{S230} (Fig. 1E). To exclude the possibility that the DAPK inhibitor affected CAMKII activity, we performed an *in vitro* kinase assay and demonstrated that the DAPK inhibitor did not interact with CAMKII (Fig. 1F). Next, we investigated pHSF1^{Ser230} and DAPK protein levels during treatment with TNF in two additional colorectal tumor cell lines. Upregulation of pHSF1^{Ser230} was observed in DLD1 and Caco2 cells (Fig. 1G). Interestingly, in normal colon epithelial cells (HCEC), HSF1 and pHSF1^{Ser230} proteins responded to the TNF-induced stress in a DAPK-independent manner (Fig. 1H).

We also investigated the level of pHSF1^{Ser230} during the exposure of HCT116 cells to another pro-inflammatory cytokine, interleukin-6. Indeed, the level of phosphorylation of HSF1 at Ser230 was not increased after treatment with interleukin-6 (supplementary material Fig. S1A), suggesting a TNF-specific effect. These findings suggest that the upregulation of pHSF1^{Ser230} is a common TNF-mediated response in colorectal tumor cells, with DAPK being the responsible upstream kinase.

DAPK interacts with HSF1 *in vitro* and *in vivo*

To further characterize the DAPK–HSF1 interaction, we created an in silico structural model of the HSF1–DAPK complex (Fig. 2A). This model shows that the side-chain hydroxyl group of Ser230 is ideally positioned to become phosphorylated by the terminal phosphoryl group of the bound ATP. In addition, the model of the complex offers a structural explanation for the requirement for a basic residue at the −3 position in DAPK recognition motifs. Arg227 of HSF1 penetrates a cleft on the DAPK surface and forms polar interactions both with the side chain of Glu100 and with the hydroxyl group of the ATP ribose ring (Fig. 2A; purple arrow). In DAPK-overexpressing HCT116 cells, we identified HSF1 with a 753.0 score range (supplementary material Fig. S1B,C) in mass spectrometric analysis, confirming that DAPK and HSF1 are able to form a stable complex upon TNF exposure *in vivo*.

An *in vitro* GST-binding assay confirmed the direct interaction of both proteins, whereby a possible interaction between the GST tag of DAPK and HSF1 was excluded. We analyzed proteins from two fractions by western blotting – the DAPK–GST bead precipitants and the corresponding supernatants containing unbound proteins. HSF1 was found in the complex with DAPK-containing beads (although some HSF1 was also detected in the supernatants), whereas GST beads alone did not precipitate HSF1 protein (Fig. 2B), indicating a direct binding of HSF1 to the catalytic domain of DAPK.

In co-immunoprecipitation experiments, overexpressed and endogenous DAPK and HSF1 showed increased complex formation following TNF treatment for 24 h (Fig. 2C; supplementary material Fig. S2A), followed by a decrease in complex formation at 48 h. Correspondingly, the cytoplasmic pHSF1^{Ser230} level was highest at 24 h, whereas in nuclear lysates the maximum level of pHSF1^{Ser230} was achieved later, between 24 and 48 h after TNF exposure (supplementary material Fig. S2B). We found a strong colocalization of endogenous DAPK and pHSF1^{Ser230} by confocal microscopy analysis at 24 h after TNF stimulation in apoptotic cells, which were characterized by fragmented chromatin (Fig. 2D). Our results indicate the existence of an interaction between HSF1 and DAPK in cell-based and in cell-free systems, and the data show that TNF is stabilizing this interaction *in vivo*.

HSF1 is a new substrate for DAPK phosphorylation *in vivo*, *in vitro* and *in silico*

To verify HSF1 as a new DAPK phosphorylation target, HCT116 cells were transfected with plasmids encoding wild-type DAPK, a

Journal of Cell Science (2014) 127, 5273–5287 doi:10.1242/jcs.157024

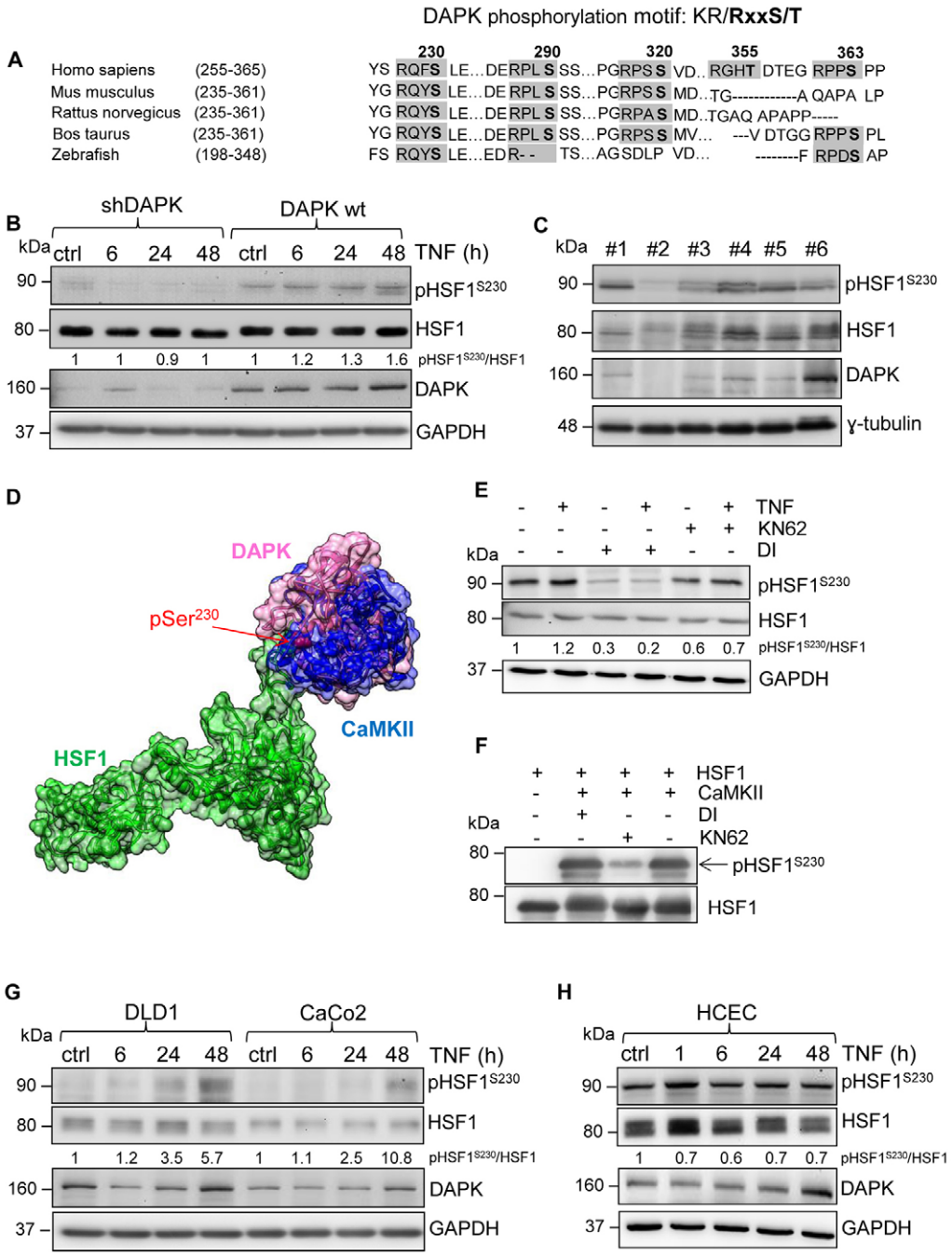

Fig. 1. See next page for legend.

K42A dead mutant and versions of DAPK containing the mutations S308A (autophosphorylation site, higher kinase activity) and S308D (lower kinase activity) (Jin et al., 2006). In an immunoprecipitation and *in vitro* kinase assay, the resulting autoradiogram demonstrated that wild-type DAPK phosphorylates HSF1 independently of TNF (Fig. 3A,B). By contrast, the catalytically dead mutant K42A does not phosphorylate HSF1. The DAPK S308A mutant had a prominent positive effect on HSF1 phosphorylation, whereas overexpression of S308D led to a significant decrease in pHSF1^{Ser230} protein levels. To verify the phosphorylated HSF1 signal, we performed direct DAPK-mediated phosphorylation of HSF1 under cell-free conditions. We incubated recombinant HSF1 and DAPK in the presence of cold ATP *in vitro* and the products of the reactions were investigated by immunoblotting with the anti-pHSF1^{Ser230} antibody. Indeed, we found that DAPK phosphorylated HSF1 at Ser230 (Fig. 3C, lane 6). Correspondingly, treatment with the DAPK inhibitor diminished the phosphorylation of HSF1 (Fig. 3C, lanes 7, 8). These results suggest that DAPK directly phosphorylates HSF1 on Ser230 *in vitro* and *in vivo*.

To better understand the interaction of the DAPK inhibitor with the DAPK–HSF1 complex (Fig. 3D), we performed structural modeling analysis. We show that the DAPK inhibitor

Journal of Cell Science

Journal of Cell Science (2014) 127, 5273–5287 doi:10.1242/jcs.157024

Fig. 1. pHSF1^{Ser230} is upregulated by TNF in colon cancer cells. (A) Peptide alignment of HSF1 from various species. Putative DAPK phosphorylation sites are boxed in gray. (B) HCT116 cells (DAPK wt) and HCT116 cells with DAPK knocked down by shRNA (shDAPK) were treated with 0.66 ng/ml TNF. At the indicated time-points, whole-cell lysates were prepared and equal amounts of protein were resolved by SDS-PAGE and probed with the specific antibodies indicated. GAPDH was used as a loading control. Ctrl, control. (C) Colorectal tumor tissue lysates were immunoblotted with antibodies as indicated. γ-tubulin was used as a loading control. (D) Interaction of the DAPK–HSF1–CaMKII complex. The catalytic domain of DAPK (PDB ID: 1JKS) was docked to HSF1 modeled using the PDB IDs 2LDU (10–123), 4DZM and 1EXU (126–203), 3K9J (200–260), 2VBC (203–310), 1Z05 (311–371), 2WLX and 3OOQ (371–529). CaMKII in its active form was modeled with the PDB ID 3KK8 as a template and was then docked to the DAPK–pHSF1^{Ser230} complex. HSF1 is shown in green, CaMKII is indicated in blue and the DAPK kinase domain is shown in pink. Phosphorylated residue Ser230 of HSF1 is shown as a red sphere. (E) HCT116 cells were treated with 10 μM KN62 (CaMKII inhibitor) or 10 μM DAPK inhibitor (DI), with or without 0.66 ng/ml TNF. At 24 h after treatment, cell lysates were resolved by SDS-PAGE and probed with the specific antibodies indicated. GAPDH was used as a loading control. (F) Recombinant HSF1–His (1 μg) was incubated with recombinant CaMKII (0.5 μg) and ATP (200 μM) in CaMKII kinase buffer in the presence of 10 μM KN62 (CaMKII inhibitor) or 10 μM DAPK inhibitor at 30°C for 30 min. Proteins were resolved by SDS-PAGE. The level of phosphorylation was determined using a specific antibody against pHSF1^{Ser230}. (G) Colorectal adenocarcinoma cell lines DLD1 and Caco2 were treated with 0.66 ng/ml TNF. At the indicated time-points, cell lysates were resolved by SDS-PAGE and probed with the specific antibodies indicated. GAPDH was used as a loading control. (H) Western blot analysis of HCEC cell lysate treated with 0.66 ng/ml TNF for the indicated times. Blots were immunoprobed with the indicated antibodies. Blots from representative experiments are shown (n=3). In all cases the ratio of pHSF1^{Ser230}:HSF1 was calculated using ImageJ and the control of each cell line was adjusted to 1.

is bound to the catalytic site of DAPK surrounded by residues Leu93, Val96, Met146, Ile160 and Asp161 in both DAPK and in the DAPK–HSF1 complex. In the DAPK–HSF1 complex, the residues Gln228, Phe229 and Glu232 of HSF1 are found in the 4 Å interface of the DAPK inhibitor. When the inhibitor is introduced, the ATP-binding site of DAPK is blocked. The conformational changes arising in DAPK due to inhibitor treatment might hinder the recognition of the residues Gln228, Phe229 and Ser230 of the HSF1 consensus motif (RXXS/T). The catalytic domain of DAPK (PDB ID: 1JKS), the inhibitor-bound conformation of DAPK and the catalytic domain with inhibitor bound to HSF1 are superimposed and presented in Fig. 3E. It was observed that conformational rearrangements occurred at the catalytic domain of DAPK upon binding of the inhibitor to the complex. Interestingly, these changes were noticeable as structural rearrangements at the DAPK-specific basic loop (residues 46–56), comprising the motif KRXXXXSRRG located at the upper lobe of the catalytic domain. The residues in this loop are highly exposed and face the catalytic site of DAPK (Temmerman et al., 2013). Besides this, there are significant structural rearrangements in the activation segment (residues 163–186), surface loops (residues 22–25 and 213–221) and in the N-terminal helix A (residues 8–12) of DAPK. These conformational rearrangements, which influence the surface region of DAPK, might possibly hinder the recognition of DAPK by its antibody and might also explain why the DAPK western blot signal was diminished under DAPK inhibitor treatment (Fig. 3C) despite equal loading (Fig. 3C, Coomassie staining).

DAPK-mediated HSF1 phosphorylation triggers TNF-induced apoptosis

Next, we studied whether TNF-induced apoptosis is an HSF1-dependent process. Transient transfection of HCT116 cells with HA–HSF1 cDNA led to 43% tumor cell death at 24 h after transfection (Fig. 4A,B), with TNF treatment further enhancing this effect to 50% apoptotic cells. Apoptosis seems to be partially mediated by caspase-3 activation (Fig. 4C). By contrast, transfection of HSF1 siRNA led to a twofold decrease in the amount of cell death under TNF – 21.2% versus ~9.2% (Fig. 4A,B). To examine the role of Ser230 phosphorylation in TNF-induced apoptosis, we transfected HCT116 cells with a non-phosphorylatable version of HSF1 (S230A) and a phosphomimetic form (S230E). Overexpression of the S230A mutant increased the apoptotic cell population (as determined by annexin V^+/PI^- staining) by twofold compared with the control (Fig. 4A, lower panel), but cell populations overexpressing S230A did not reach the apoptosis level induced by expression of wild-type HSF1 – 20% versus 37%, respectively. Nevertheless, TNF exposure of S230A-transfected cells further increased the apoptotic cell population to ~37%. Unexpectedly, S230E did not result in a greater apoptotic response than S230A. By performing computational predictions, we found that this residue affects the ability for nuclear import of HSF1. A nuclear localization signal (NLS) prediction suggests that Ser230 is part of a bipartite NLS sequence spanning residues 201–232. Interestingly, a S230E mutation is predicted to reduce the strength of the NLS significantly, whereas a S230A mutation has almost no effect (the NLS scores for wild type, S230A and S230E are 4.4, 4.6 and 3.6, respectively). These data suggest that although phosphorylation on Ser230 of HSF1 seems to play a crucial role in promoting apoptosis, other putative sites in HSF1 could be involved in DAPK phosphorylation.

The regulatory domain of HSF1 ensures its pro-apoptotic effect

The human HSF1 contains seven potential DAPK phosphorylation motifs different from Ser230 that were not included on the peptide microarray: Thr97, Thr120, Ser136, Ser290, Ser320, Thr355 and Ser363 (Fig. 5A). Next, we aimed to find out which amino acid(s) could be involved synergistically in phosphorylation by DAPK. Based on structural analysis of the Thr97 site, we excluded this amino acid as a candidate phosphorylation target, because Thr97 is not accessible and is hidden inside the globular structure (data not shown). Further bioinformatic screening was limited owing to the lack of an experimental structure for the downstream sequence region. It is known that Thr120 and Ser136 are adjacent to residues that are involved in transcriptional repression (Chu et al., 1996; Wang et al., 2006), and they were therefore excluded from further investigation. More intriguing was a motif downstream of Ser230 containing four potential DAPK-phosphorylation sites – Ser290, Ser320, Thr355 and Ser363 – all of which are located within the HSF1 regulatory domain. We created a mutant with a deletion of this region [cluster deletion mutant (CDM), amino acids 250–370; Fig. 5A, lower panel; Fig. 5B]. To verify that the globular domain of HSF1 was not damaged by this 121-amino-acid deletion, we performed immunofluorescence analysis. We identified that the CDM did not affect HSF1 nuclear translocation (Fig. 5C). Some of the CDM-transfected cells that clearly demonstrated fragmented chromatin as a marker of apoptosis showed colocalization of DAPK and HSF1-CDM at 12 h after TNF exposure.

Journal of Cell Science (2014) 127, 5273–5287 doi:10.1242/jcs.157024

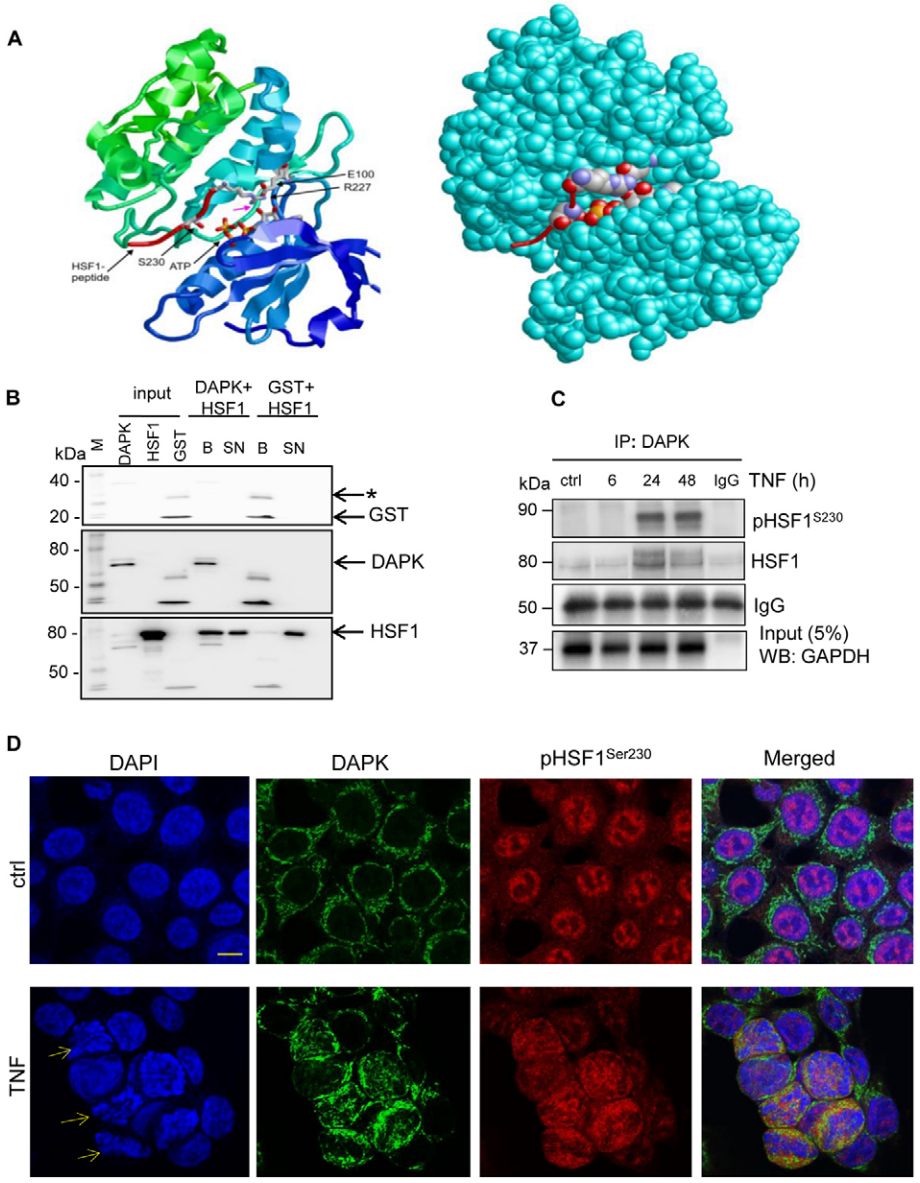

Fig. 2. DAPK interacts with HSF1 *in vivo* and *in vitro*. (A) A model of the DAPK kinase domain in complex with a substrate peptide comprising HSF1 residues 227–233. Left panel, the backbone topology of DAPK is shown in shades from blue to green and the bound ATP is shown in stick presentation (coloring according to the atom types). The key residues Arg227 and Ser230 of the HSF-1 peptide and Glu100 of DAPK are shown in stick presentation. The Ser230 sidechain is located in proximity to the terminal phosphoryl group of the ATP and Arg227 interacts with Glu100 and the ribose oxygens of ATP (magenta arrow). Right panel, space-filled representation of the complex (same view as in the left panel). The kinase domain is shown in cyan and the key interacting residues are colored according to their atom type. (B) Recombinant DAPK–GST catalytic domain or recombinant GST proteins, immobilized on glutathione–agarose beads, were incubated with equal amounts of recombinant HSF1–His in binding buffer. Western blotting indicated that the proteins precipitated with glutathione–agarose beads ('B') and 10% of unbound target protein from the supernatant (SN) fraction using specific antibody. After probing with the first antibody, the membrane was stripped and reblotted with the next antibody. The asterisk indicates a nonspecific band for the GST antibody. M, biotinylated molecular mass marker. (C) HCT116 cells were transiently transfected with DAPK–HA (2 μg) construct. The transfection medium was changed after 6 h, and the cells were supplied with fresh TNF-containing medium. Cells were harvested at the indicated time-points after TNF stimulus. DAPK was immunoprecipitated (IP) using a specific antibody, and the bound products were immunoblotted with the indicated antibodies. IgG beads were incubated with DAPK-specific antibody and used as a negative control. Input controls (5% of the extract used for immunoprecipitation) are shown in the lower panel. Blots from representative experiments are shown (n=3). Ctrl, control. (D) HCT116 cells were treated with 0.66 ng/ml TNF for 24 h and fixed with 3.7% paraformaldehyde. The subcellular location of endogenous pHSF1^{Ser230} (red) and DAPK (green) was analyzed by confocal microscopy. DAPI staining (blue) was used to identify nuclei. Arrows indicate fragmented chromatin. Scale bar: 12 μm. n=3 for all experiments.

Next, we examined the effects of CDM on TNF-induced apoptosis. CDM-overexpressing cell populations showed only 16.6% apoptotic cells compared with 43% in cells transfected with wild-type HSF1 (Fig. 4A; Fig. 5D,E). TNF treatment of CDM-overexpressing cells further enhanced apoptosis to ~20%, yet it was remarkably lower than the amount of apoptosis observed in TNF-treated cells overexpressing wild-type HSF1 (~50%, Fig. 4A,B). These data indicate that the additional DAPK phosphorylation motifs in the regulatory domain of HSF1 might be necessary for further transduction of the DAPK-mediated apoptotic signal.

Journal of Cell Science (2014) 127, 5273–5287 doi:10.1242/jcs.157024

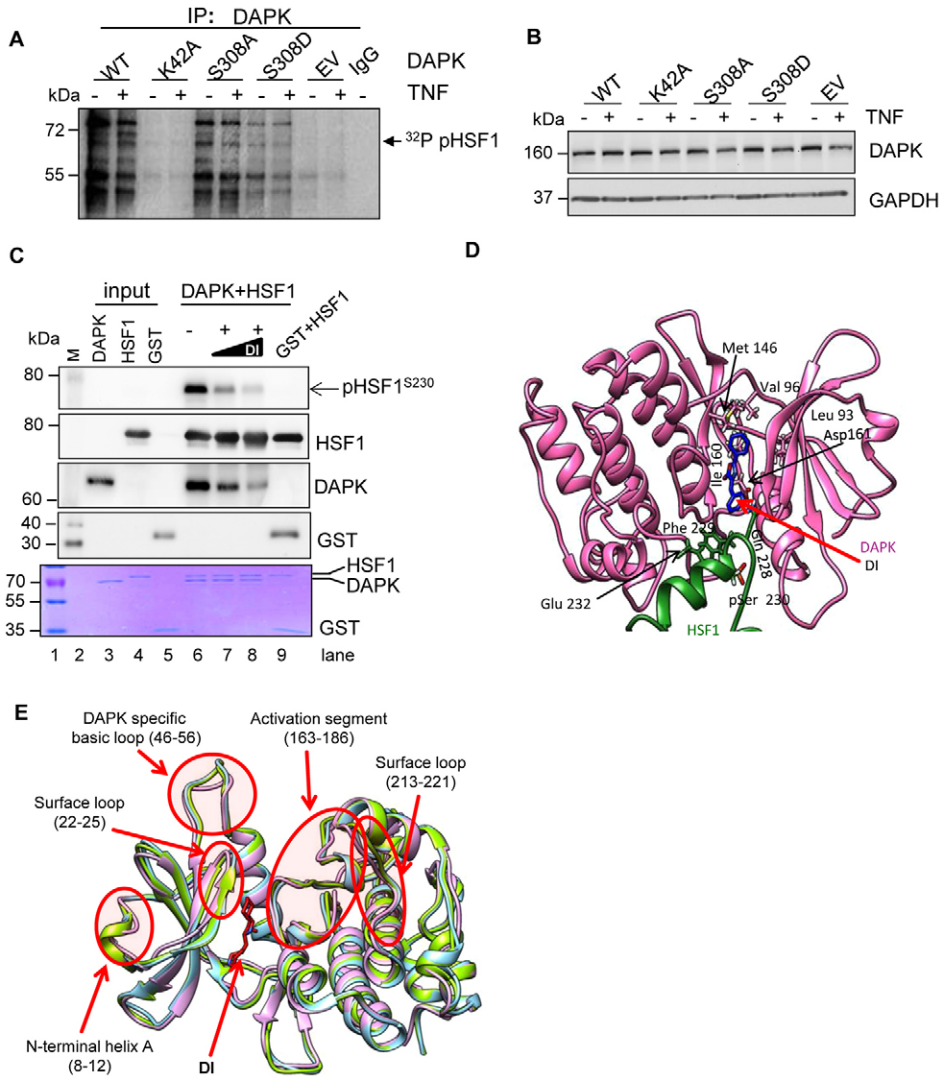

Fig. 3. DAPK phosphorylates HSF1 *in vivo*, *in vitro* and in silico. (A) HCT116 cells were transfected with wild-type (WT) DAPK, DAPK K42A dead mutant, S308A and S308D mutants. Empty vector (EV) was used as a negative control. Immunoprecipitation (IP) was performed using a DAPK-specific antibody. Magnetic beads were washed and incubated with recombinant HSF1–His (1 μg) in the presence of 7.5 μCi [γ-^{32}P]ATP and 200 μM ATP in DAPK kinase buffer for 30 min at 30˚C. The samples were subjected to separation by SDS-PAGE, followed by autoradiography. (B) Protein expression level of wild-type DAPK and K42A, S308A and S308D mutants and empty vector in transfected HCT116 cells was assessed by western blotting using a DAPK-specific antibody. GAPDH was used as a loading control. (C) Recombinant HSF1–His (1 μg) was incubated with a GST-tagged catalytic domain of DAPK (0.5 μg) and ATP (200 μM) in DAPK kinase buffer, in the absence or presence of DAPK inhibitor (DI; 10 and 30 μM) at 30˚C for 30 min. The products of the *in vitro* phosphorylation reaction were divided into two parts. Half was resolved by SDS-PAGE and analyzed by western blotting, and the other half was used as a loading control. One membrane was used for all indicated antibodies. The lower panel represents Coomassie Brilliant Blue R-250 staining and indicates equal protein loading. The first lane contains a prestained protein marker (PeqGold V, Peqlab); the second lane contains a biotinylated marker ('M'). Input indicates the amount of protein used in the *in vitro* phosphorylation reaction. Incubation of recombinant GST and HSF1–His in the presence of cold ATP was used as a negative control. All experiments were repeated at least three times, and representative data are shown. (D) Interface of the HSF1–DAPK complex with the DAPK inhibitor. HSF1 and DAPK are shown in green and pink, respectively. DAPK inhibitor is shown in blue. Residues within 4 Å of the inhibitor are shown in stick representation. (E) Conformational changes in the DAPK catalytic domain upon inhibitor binding. Superposed structures of the DAPK catalytic domain available in PDB ID: 1JKS (blue), inhibitor-bound conformation of DAPK (green) and catalytic domain with inhibitor bound to HSF1 (pink) are superposed. DAPK inhibitor is shown in stick representation. Regions in DAPK showing conformational rearrangements are highlighted (red circles).

Detailed mapping of phosphorylation sites within the regulatory domain might help us to understand the fine-tuning of the DAPK-mediated HSF1 signal transduction cascade in the future.

DAPK is a transcriptional target of HSF1

As we have shown previously, endogenous DAPK mRNA expression increases up to 2.0-fold upon exposure to TNF (Bajbouj et al., 2009). Interestingly, we found a single fully matching HSF1-binding motif (5′-TTCXXGAA-3′) in the human DAPK promoter (http://www.cbrc.jp/research/db/TFSEARCH.html) (Fig. 6A). To investigate whether HSF1 can lead to the transactivation of the DAPK promoter, we employed a *Gaussia* luciferase reporter assay. We transfected HEK293 cells with the dual GLuc/SeAP-ON DAPK reporter clone and corresponding

Journal of Cell Science (2014) 127, 5273–5287 doi:10.1242/jcs.157024

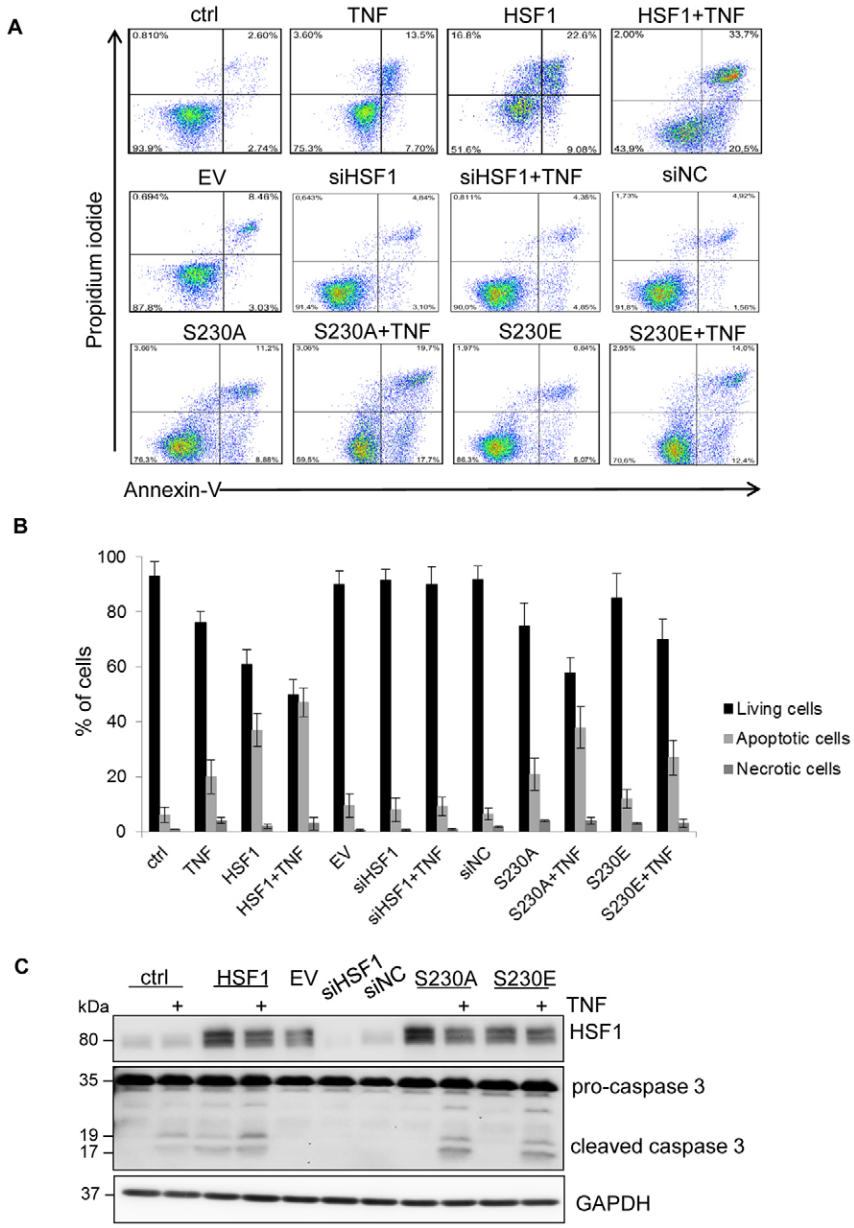

Fig. 4. HSF1 is triggering DAPK-dependent apoptosis by TNF. (A) Scatter plots of flow cytometric analysis of annexin-V and propidium iodide staining of untreated HCT116 cells (ctrl), HCT116 cells subjected to 0.66 ng/ml TNF treatment (TNF), HCT116 cells transfected with either HSF1–HA cDNA (HSF1) or with HSF1 S230A or S230E mutant plasmids. pHACE-HA cDNA was used for HCT116 cell transfection as an empty vector (EV). Also analyzed were HCT116 cells transfected with either HSF1 siRNA (siHSF1) or scrambled siRNA, used as negative control (siNC). TNF treatment was performed at 6 h after transfection. The apoptosis rate was assessed as the sum of the lower right quadrant (early apoptosis) and upper right quadrant (late apoptosis). (B) Quantification of the mean annexin-V and propidium iodide fluorescence of the cell population (n=3; ±s.e.m.). (C) HCT116 cells were transfected with 2 µg of wild-type HSF1–HA or S230A and S230E mutants. Empty vector was used as a negative control. Alternatively, 100 nM HSF1 siRNA or scrambled siRNA was transfected. At 6 h after transfection, fresh TNF-containing medium (or medium without TNF) was added. At 24 h after TNF incubation, cells were harvested, lysates were resolved by SDS-PAGE and probed with the specific indicated antibodies. GAPDH was used as a loading control. Blots from representative experiments are shown (n=3).

control plasmids. As shown in Fig. 6B, TNF induced a tenfold activation of the DAPK promoter within 24 h. Co-transfection of the GLuc DAPK promoter plasmid with the HSF1 expression construct resulted in a significant increase in the activation of the DAPK promoter upon treatment with TNF. Next, we performed chromatin immunoprecipitation (ChIP) to verify DAPK as a transcriptional target of pHSF1^{Ser230}. The PCR fragments amplified from the immunoprecipitated DNA–protein complexes revealed that pHSF1^{Ser230} interacts with an HSE-containing chromatin fragment. This binding was further increased after TNF stimulation from 1.3 to 2.3-fold compared with control (Fig. 6C). The peak was observed at 48 h after TNF treatment, in line with the enrichment of pHSF1^{Ser230} protein levels in the nuclear compartment (supplementary material Fig. S2B). One sequence region upstream and one downstream of HSE were analyzed as negative controls (Fig. 6D). Quantitative PCR amplification demonstrated that motifs without a complete HSE do not show any augmentation of this DNA–protein association following treatment with TNF (Fig. 6E).

These data suggest an HSF1-mediated transcriptional activation of the DAPK promoter under conditions of TNF stress. This leads to the hypothesis that DAPK phosphorylates HSF1, which consequently binds to the DAPK promoter, forming a positive-feedback loop for DAPK regulation and promoting apoptosis in colorectal tumor cells under mild inflammatory stress.

Because we suggested that HSF1 as transcription factor can switch from a pro-survival to a pro-apoptotic pathway, we next tested the expression level of known HSF1 target genes, such as HSP70, HSP90 and BAG3 (Jacobs and Marnett, 2009; Morimoto et al., 1996; Wu, 1995). Western blot analyses indicated equal protein expression of these three pro-survival factors under exposure to TNF (supplementary material Fig. S2C), confirming that under mild stress HSF1 action could be redirected.

Journal of Cell Science (2014) 127, 5273–5287 doi:10.1242/jcs.157024

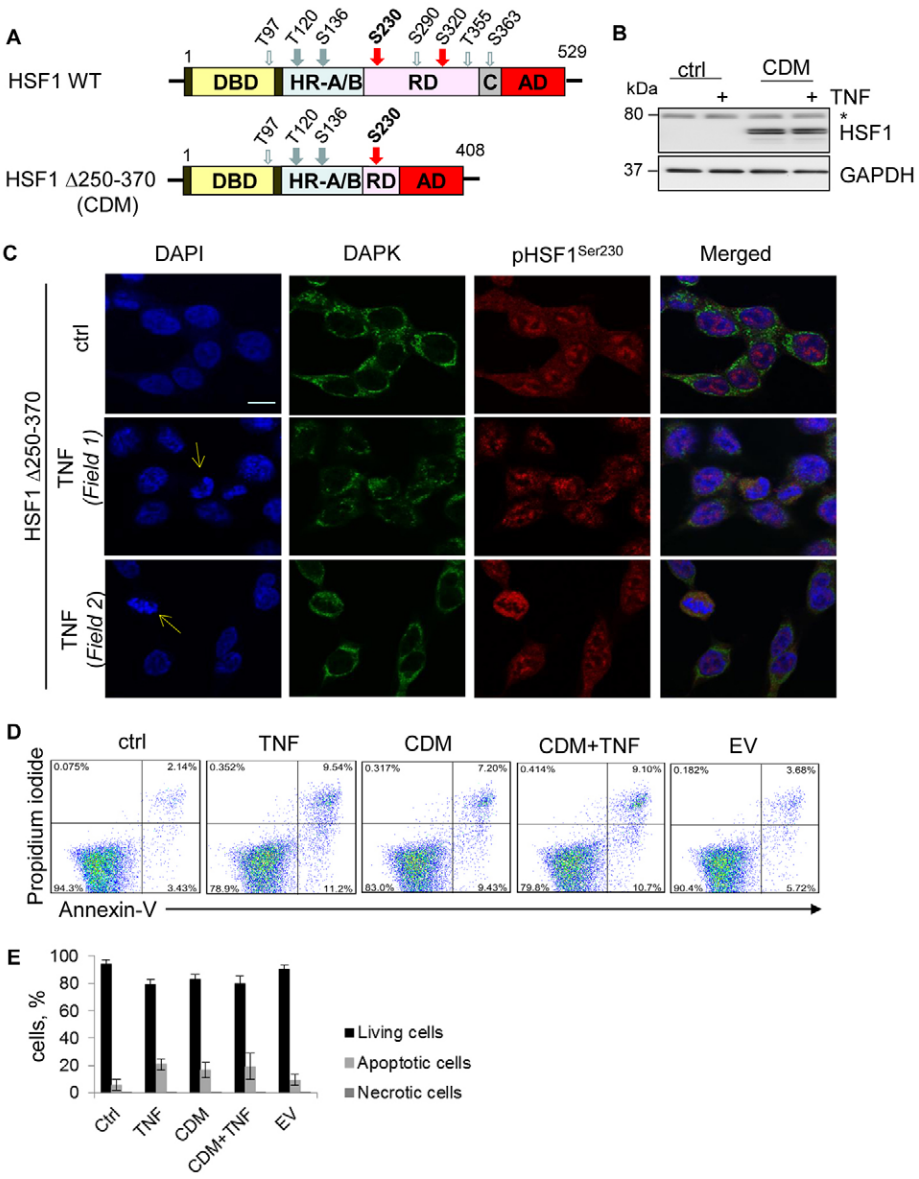

Fig. 5. The regulatory domain of HSF1 is involved in the pro-apoptotic response to TNF. (A) Upper panel, functional domains and potential DAPK phosphorylation motifs in human HSF1. DBD, DNA-binding domain; HR-A/B, harbour domain/leucine zipper trimerization domain; RD, regulatory domain; C, heptad repeat region C; AD, activation domain. Blue arrows show transcription-inhibitory phosphorylation; red arrows show transcription-inducing phosphorylation; white arrows indicate residues for which phosphorylation has unknown effects on gene transcription. Lower panel, schematic representation of the HSF1 cluster deletion mutant (CDM), containing partially excluded sequence of the regulatory domain (amino acids 250–370). WT, wild type. (B) HCT116 cells were transfected with 2 μg of HSF1-CDM–HA construct. Equal amounts of protein were resolved by SDS-PAGE and probed with the HSF1-specific antibody. The asterisk indicates endogenous HSF1. GAPDH was used as a loading control. Ctrl, control. (C) HCT116 cells were co-transfected with 1 μg of HSF1-CDM–HA and DAPK–FLAG constructs and treated with 0.66 ng/ml of TNF for 12 h. The subcellular localization of exogenous pHSF1^{Ser230} (red) and DAPK (green) was visualized by confocal microscopy. DAPI staining (blue) was used to identify nuclei. Arrows indicate fragmented chromatin. Scale bar: 12 μm. n=2 for all experiments. (D) Scatter plots of flow cytometric analysis of annexin-V and propidium iodide staining of untreated HCT116 cells (Ctrl), HCT116 cells subjected to TNF treatment (TNF) and HCT116 cells transfected with either HSF1-CDM–HA cDNA (CDM) or empty vector (EV). TNF treatment was performed at the same time for all samples, 6 h after cDNA transfection, for 24 h. The apoptosis rate is determined as the sum of the lower right quadrant (early apoptosis) and upper right quadrant (late apoptosis). (E) Quantification of the mean annexin-V and propidium iodide fluorescence of the cell population (n=3; ±s.e.m.).

Correlation of DAPK and pHSF1^{Ser230} protein expression in colorectal cancer tissues

To investigate the protein interaction between DAPK and pHSF1^{Ser230} in human colorectal tissues, we performed immunohistochemistry using specific antibodies against DAPK and pHSF1^{Ser230} on formalin-fixed and paraffin-embedded tissue samples. In normal colonic mucosa, pHSF1^{Ser230} expression was evident in both cytoplasmic and nuclear compartments, and was especially predominant in the crypt areas with a high rate of turnover (supplementary material Fig. S3A). DAPK expression in the normal mucosa was relatively weak and confined to the cytoplasm of the most superficial crypts and epithelium (supplementary material Fig. S3A). After microscopic evaluation of 53 colorectal cancer tissue samples, we found that tumors showed proportional correlation between the expression of the two proteins (R_P=0.379 and P=0.005) (supplementary material Fig. S3C). Using the median values of immunostaining as a cut-off point for dividing the tumors into high versus low expression of DAPK and pHSF^{Ser230}, we found high DAPK and high pHSF1^{Ser230} staining in eight (15.2%) tumors (Fig. 7B,C), low DAPK1 and low pHSF1^{Ser230} staining in 28 (52.8%) (Fig. 7E,F), high DAPK1 and low pHSF1^{Ser230} staining in 12 (22.6%) tumors (Fig. 7H,I), and low DAPK and high pHSF1^{Ser230} staining in five (9.4%) tumors (Fig. 7K,L). We found that the group expressing low levels of DAPK and pHSF1^{Ser230} was the most aggressive one, with 17 of 28 (60.7%) tumors showing lymph node metastasis. The other three groups did not differ regarding their nodal status and showed positive lymph nodes in <30% of cases (P=0.026) . There was no significant correlation of these four groups with sex, age, localization, tumor grade, T stage or UICC stage.

Furthermore, we investigated several colorectal cancer samples using conventional tissue slides instead of tissue microarray (TMA) and in two of them we found a gradual increase in DAPK and pHSF1^{Ser230} expression from tumor centers towards the invasion front, suggesting a distinct expression pattern associated with the invasion process (Fig. 7M,N).

DISCUSSION

It is known that DAPK acts as a tumor suppressor or oncogene depending on the cellular context and experimental settings.

Journal of Cell Science (2014) 127, 5273–5287 doi:10.1242/jcs.157024

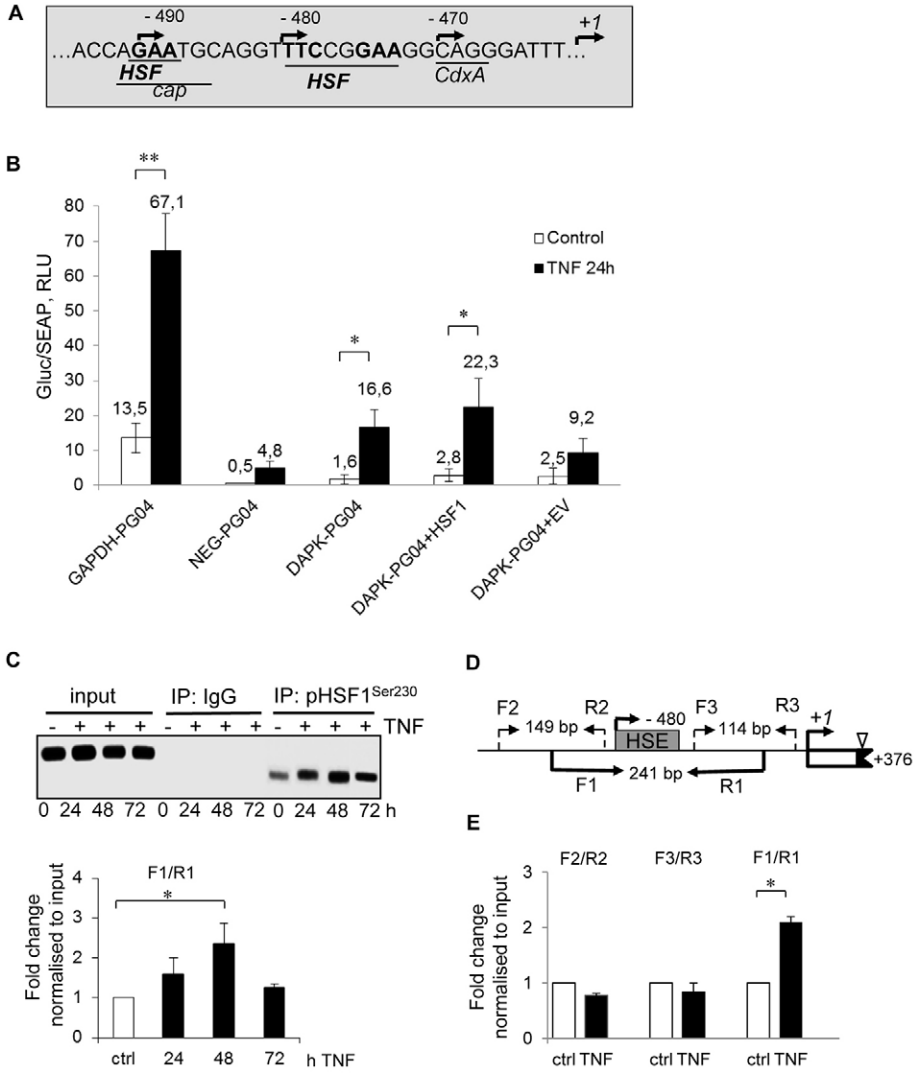

Fig. 6. pHSF1^{Ser230} binds to the DAPK promoter. (A) Regulatory elements in the proximal human DAPK promoter. The numbering of nucleotides is relative to the transcriptional start site (+1). (B) HEK293 cells were transiently transfected with 2 μg of dual *Gaussia* Luciferase (GLuc)/secreted alkaline phosphatase (SeAP) constructs: GAPDH-PG04 (positive control), NEG-PG04 (negative control), DAPK promoter-PG04, HSF1–HA and empty vector (EV, pHACE, 2 μg) constructs. All luciferase assay results are expressed as relative light units (RLU) and presented as a ratio of the mean GLuc reporter to secreted alkaline phosphatase luminescence signals. The RLU values obtained from co-transfected cell samples were normalized to those co-transfected with the DAPK promoter-PG04 reporter and the pHACE empty vector. Experiments were performed in triplicate and repeated three times; representative experiments are depicted. Data show the mean±s.d.; *$P<0.05$; **$P<0.01$ (unpaired two-tailed *t*-test). (C) Upper panel, ChIP assay using anti-pHSF1^{Ser230} was performed on HCT116 cell lysates. The DAPK promoter was identified by PCR amplification of the DNA fragments precipitated with anti-pHSF1^{Ser230} antibody. Input represents one-tenth of cleared supernatant. IgG immunoprecipitates (IP) were used as negative controls. Lower panel, immunoprecipitated DNA and input DNA were quantified by real-time PCR with primers specific for the HSE in the DAPK promoter (F1/R1). Data are represented as the mean±s.d.; *$P<0.05$ (unpaired two-tailed *t*-test). Ctrl, control. (D) Schematic representation of the primers designed for chromatin immunoprecipitation. The HSE in the DAPK promoter is illustrated, and the HSE region was amplified by using the F1/R1 primers. Negative control regions without HSE motifs are amplified using the upstream F2/R2 or downstream F3/R3 primer pairs. The boxed white region indicates the primary transcript, and the black region indicates the ATG codon as the start of translation. (E) Immunoprecipitated and input DNA were quantified by real-time PCR with HSE-specific primers (F1/R1) and HSE-nonspecific primers (F2/R2 and F3/R3) in the DAPK promoter after 48 h of TNF treatment. Data are represented as the mean±s.d.; *$P<0.05$ (unpaired two-tailed Student's *t*-test). All experiments were repeated at least three times.

Thus, a better understanding of the DAPK interactome will help to decipher this antagonistic functional duality and to define DAPK as a potential biomarker in cancer. We have shown previously that DAPK plays an anti-inflammatory role in normal intestinal epithelial cells without inducing cell death (Chakilam et al., 2013). Otherwise, under mild pro-inflammatory stress with TNF there is DAPK-dependent apoptosis in colon cancer cells through the activation of p38 (Bajbouj et al., 2009) or LIMK (Ivanovska et al., 2013), which is not induced by IL-6 (Bajbouj et al., 2009). To identify other potential interaction partners of DAPK in response to TNF we performed a phosphopeptide microarray. Among the TNF-induced phosphorylated targets we searched for those with a DAPK-specific K/RXXS/T and KRRXXS/T consensus motif. Interestingly, the classical anti-apoptotic HSF1 protein was highly phosphorylated on Ser230 in response to TNF. In our peptide array, three other HSF1 peptides

Journal of Cell Science (2014) 127, 5273–5287 doi:10.1242/jcs.157024

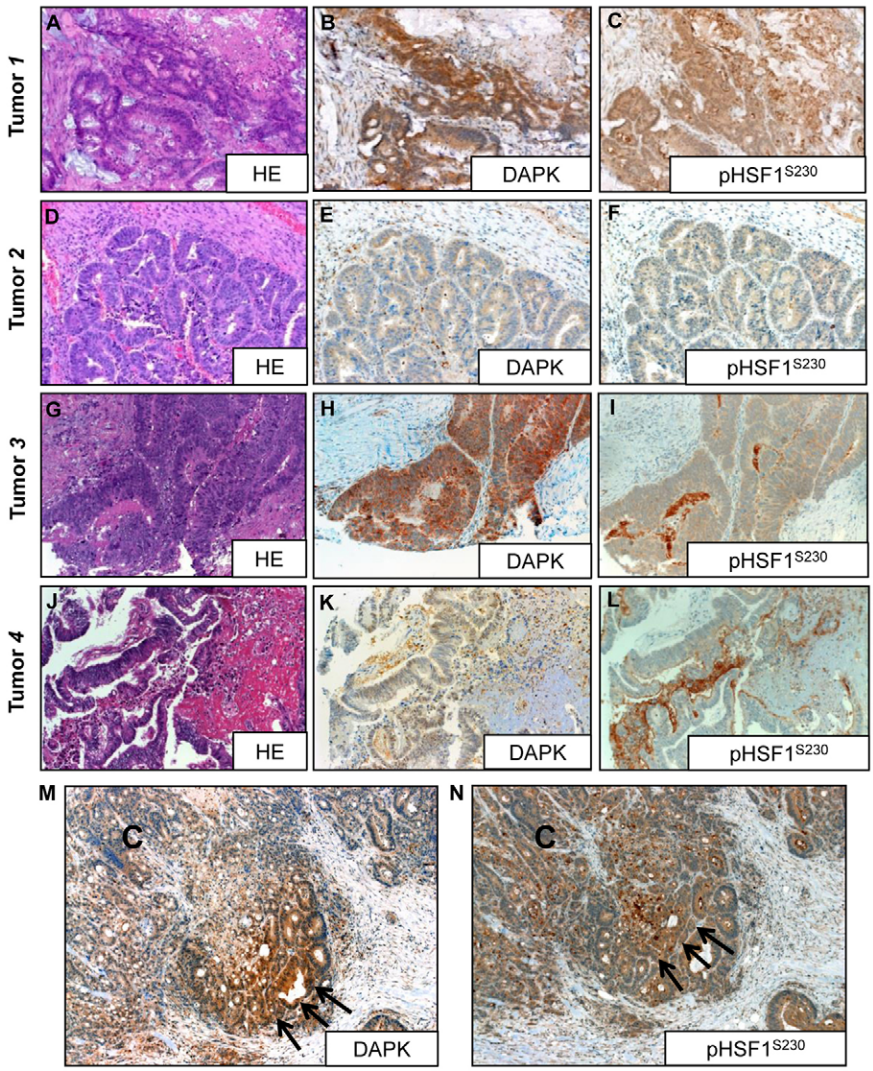

Fig. 7. Pattern of DAPK and pHSF1^{Ser230} expression in human colorectal tumor tissue as determined by immunohistochemistry on formalin-fixed paraffin-embedded tissue samples. Tumor 1. (A) Hematoxylin and eosin (HE)-staining of colorectal cancer showed a cribriform pattern and mucous secretion. (B) Immunohistochemical analysis using the DAPK-specific antibody indicated moderate to strong cytoplasmic expression of DAPK in the tumor cells. (C) Immunohistochemical analysis using the pHSF1^{Ser230}-specific antibody showed moderate expression of pHSF1^{Ser230} in both the cytoplasm and the nuclei of tumor cells. Tumor 2. (D) HE staining of rectal cancer showed a predominant tubular pattern. (E) Immunohistochemical analysis using the DAPK-specific antibody indicated complete absence of cytoplasmic DAPK. (F) Immunohistochemical analysis using the pHSF1^{Ser230}-specific antibody demonstrated lack of pHSF1^{Ser230} in the tumor cells. Tumor 3. (G) HE staining of colorectal cancer showed poorly formed fused glands and extensive necrosis. (H) Strong cytoplasmic expression of DAPK is seen in this sample. (I) The same tumor lacked pHSF1^{Ser230} expression (except for nonspecific staining within secretion). Tumor 4. (J) HE staining of moderately differentiated colorectal carcinoma showed dilated glands and necrosis. (K) DAPK was not expressed in the cytoplasm of this tumor (faint non-specific nuclear staining). (L) The same sample showed pHSF1^{Ser230} expression within the apical cytoplasm of tumor cells. (M) This conventional sample showed a gradual increase in DAPK expression from the tumor center (upper left, 'C') to the invasion front (lower right, arrows). (N) The same sample showed a similar pattern for pHSF1^{Ser230} (as for DAPK in M). Original magnification for all photomicrographs is ×200.

corresponding to Thr142, Ser303 and Ser307 sites were spotted; however, they did not respond to TNF treatment. Among these HSF1 motifs only the Ser230-containing peptide was recognized as a DAPK phosphorylation motif. Therefore, in our study, we focused on Ser230 – one of the key HSF1 phosphorylation sites. The active Ser230 site, located in the regulatory domain, is constitutively and stress-dependently phosphorylated and required for transactivation of HSF target genes (Holmberg et al., 2001).

The bioinformatics modeling together with co-immunoprecipitation and co-immunofluorescence studies supported the hypothesis that DAPK binds to HSF1 under conditions of TNF stress in colon cancer cells. We also found a direct DAPK–HSF1 interaction in a cell-free model. We proved that DAPK phosphorylates HSF1 by employing the kinase-dead K42A mutant, inactive S308D protein kinase form and constitutively active S308A DAPK constructs in a radioactive kinase assay. The depletion of the DAPK protein by specific short hairpin (sh)RNA or the inhibition of its catalytic activity by its specific inhibitor does not promote HSF1 phosphorylation on Ser230. In order to verify whether Ser230 of HSF1 is a target site for DAPK, we performed an *in vitro* phosphorylation assay with DAPK and HSF1 recombinant proteins and monitored the phosphorylation changes by using a phospho-site-specific antibody. Finally, we confirmed a direct DAPK-mediated phosphorylation event affecting HSF1 Ser230.

Next, we examined whether pHSF1^{Ser230} phosphorylation is involved in DAPK-dependent induction of apoptosis under conditions of mild TNF stress. Here, we demonstrate that DAPK-dependent HSF1 phosphorylation on Ser230 was associated with the induction of apoptosis, because both the expression of the non-phosphorylatable S230A mutant and the depletion of HSF1 by RNA-interference-mediated knockdown led to an attenuation of TNF-induced apoptosis. However, the hyperphosphorylated S230E form failed to increase cell death. Based on a computational analysis of the NLS region in HSF1, we suggest that this Ser230 mutation reduces the strength of the NLS and hence negatively affects shuttling to the nucleus. This might indicate the sensitivity of the Ser230 site to changes induced by mutagenesis as previously reported (Edmondson et al., 2002). In addition, multiple phosphorylation of the regulatory domain of HSF1 downstream of Ser230 might increase the induction of apoptosis, because the deletion of this region sufficiently attenuated apoptosis in our study. There seems to be some ambiguity regarding the pro- and anti-apoptotic functions of HSF1. On the one hand, targeted disruption of HSF1

Journal of Cell Science (2014) 127, 5273–5287 doi:10.1242/jcs.157024

has been found to abolish protection against heat-induced apoptosis (McMillan et al., 1998). On the other hand, expression of a constitutively transactivating HSF1 mutant remarkably enhances Fas-induced apoptosis (Tran et al., 2003). Our observations suggest that under mild inflammatory stress DAPK-dependent phosphorylation of HSF1 on Ser230 surprisingly promotes apoptosis. HSF1 transcriptional activity is amplifying in response to various environmental signals and its increased activation in cancer cells leads to the increased expression of HSPs or other target genes (Morimoto, 1998) that contain HSE elements in their promoters (Trinklein et al., 2004). However, in our study, the protein expression of HSF1 pro-survival targets such as HSP70, HSP90 and BAG3 was not induced by TNF, indicating that HSF1 is also able to activate an alternative signaling pathway through binding to the promoters of pro-apoptotic genes. Interestingly, we found an HSF1-binding site in the DAPK promoter by using the TFSearch database. Thus, we further examined whether the Ser230 phosphorylation is accompanied by an enhanced transcriptional competence of the DAPK promoter. By using a luciferase reporter assay and ChIP, we demonstrated a direct binding of $pHSF1^{Ser230}$ to the HSE in the DAPK promoter region in response to TNF, increasing the DAPK mRNA transcription. In addition to the few experimentally verified transcription factors known to regulate DAPK (Benderska and Schneider-Stock, 2014), we have identified HSF1 as a novel one. Recently, it has been shown that the HSF1-regulated transcriptional program is specific to highly malignant cells and distinct from the heat shock scenario (Mendillo et al., 2012). Our findings strongly support this idea that HSF1 function is not restricted to heat shock signaling only.

By studying human colon cancer tissues, we observed that the immunohistochemical protein expression of DAPK and $pHSF1^{Ser230}$ was significantly correlated. Tumors with high DAPK expression showed high $pHSF1^{Ser230}$ expression and vice versa. The reduced HSF1 expression in cancer tissue might be due to different oncogenic mechanisms occurring in colorectal cancer (Min et al., 2007), whereas DAPK loss might be associated with the silencing of its transcription by promoter methylation (Mittag et al., 2006). Grouping of the patients based on expression level of DAPK and $pHSF1^{Ser230}$ proteins demonstrated an interesting finding associated with tumor aggressiveness – tumors that have high expression of both proteins show low frequency of lymph node metastases in comparison with those that have low levels of DAPK and $pHSF1^{Ser230}$ expression [28.6% versus 60.7% ($P=0.026$), respectively]. Unexpectedly, we did not observe apoptotic markers [caspase 3 and M30 (antibody against a cytokeratine 18 epitope)] in TMA immunohistochemical analysis. If the $pHSF1^{Ser230}$–DAPK complex induces apoptosis, why are colon cancer cells that coexpress $pHSF1^{Ser230}$ and DAPK not apoptotic? The general situation in tissues obviously is more complex than that in an *in vitro* model, owing to the tumor microenvironment. Our finding is consistent with the known DAPK function as a metastasis suppressor (Chen et al., 2014). As DAPK is also known to suppress migration, the role of the $pHSF1^{Ser230}$–DAPK complex in migration and invasion in the tissue network has to be elucidated in the future. The gradual increase in the amount of the protein complex at the invasion front seems to be promising in this regard.

On the basis of our data, we propose the following working model (Fig. 8) – TNF induces and stabilizes a DAPK-dependent HSF1 phosphorylation on Ser230, followed by activation of DAPK mRNA transcription through direct binding of $pHSF1^{Ser230}$ to the DAPK promoter. This suggests a positive-feedback loop for DAPK regulation under conditions of mild inflammatory stress. We show for the first time that using a natural sensitizer such as TNF at a physiological low concentration in colon cancer cells could lead to a redirection of HSF1 signaling, mediated by DAPK, from a pro-survival to a pro-apoptotic pathway.

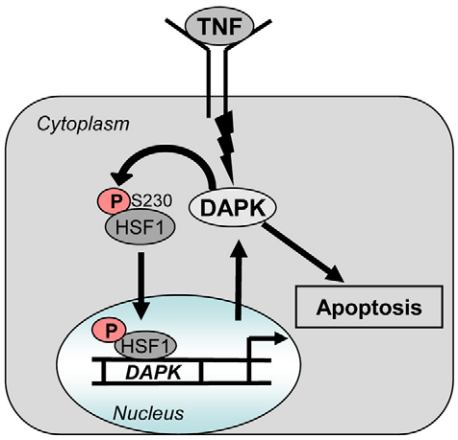

Fig. 8. Model for the DAPK–HSF1 interaction forming a positive-feedback loop in TNF-induced apoptosis. Following exposure to the TNF stimulus, HSF1 is activated and undergoes multisite phosphorylation. DAPK phosphorylates HSF1 at Ser230, which is crucial for further signal transduction within its regulatory domain, followed by its nuclear translocation. In the nucleus, HSF1 binds to the HSE in the DAPK promoter and initiates DAPK mRNA expression. As a result of this positive-feedback mechanism, the amount of pro-apoptotic DAPK in the cytoplasm increases, which leads to cell death in colon cancer cells.

MATERIALS AND METHODS

Cell culture, drugs and treatment

Human colorectal HCT116, DLD1 and Caco2 tumor cells were maintained in RPMI (HEK293 cells in DMEM) with 10% fetal bovine serum, supplemented with 1% penicillin-streptomycin. HCEC cells were maintained as described previously (Chakilam et al., 2013). Cell lines were authenticated using Multiplex Cell Authentication by Multiplexion (Heidelberg, Germany) as described previously (Castro et al., 2013). A stable cell line expressing DAPK shRNA was generated as described previously (Gandesiri et al., 2012). Cells were cultured for 6–72 h in either normal medium or medium containing TNF (Immunotools, Friesoythe, Germany; 0.66 ng/ml) and incubated in a 5% CO_2 atmosphere at 37℃. Cells were routinely monitored for *Mycoplasma* and were free from infection. The MTT assay to determine cell viability was performed as described previously (Gandesiri et al., 2012). The optimal concentrations of inhibitors and cytokines are as follows: 10 µM DAPK inhibitor 2-phenyl-4-(pyridine-3-ylmethylidene)-4,5-dihydro-1,3-oxazol-5-one (Molport, Riga, Latvia); 10 µM KN-62 (Biaffin, Kassel, Germany); 100 ng/ml rIL-6 (Immunotools, Germany). Stock solutions were dissolved in DMSO and diluted in medium to achieve the appropriate concentration.

Immunoblotting and immunoprecipitation

Cells were lysed either with urea lysis buffer (for western blotting) or with RIPA buffer (for immunoprecipitation). Protein concentration was determined by using a Bio-Rad Dc Protein Assay (BioRad, Hercules, CA). Equal amounts of lysates (600–900 µg) were incubated with specific antibodies immobilized on 50 µl of magnetic Protein G beads overnight at 4℃ (IP Dynabeads Kit, Invitrogen, Carlsbad, CA), resolved on SDS-PAGE and analyzed by western blotting. Antibodies used in this

study were as follows: rabbit polyclonal anti-HSF1 (Cell Signaling Technology, Danvers, MA), rabbit polyclonal anti-pHSF1^{Ser230}, goat polyclonal anti-BAG3, mouse monoclonal anti-HSP90 and mouse monoclonal anti-HSP70 (all from Santa Cruz Biotechnology, Santa Cruz, CA), mouse monoclonal anti-DAPK (BD Biosciences, San Diego, CA), rabbit polyclonal anti-caspase-3 and rabbit monoclonal anti-histone-3 (Cell Signaling Technology), mouse monoclonal anti-γ-tubulin (Abcam, Cambridge, UK), HRP-conjugated anti-GAPDH (Abnova, Heidelberg, Germany) and mouse monoclonal anti-GST (Thermo Fisher Scientific, Bonn, Germany). ImageJ software (v.1.45s) was used for quantification of band intensities.

Subcellular fractionation

Cells were collected by scraping after washing with cold PBS and were centrifuged on a Megafuge 16R (Thermo Scientific) supplied with a TX-400 rotor at 188 ***g*** for 5 min at 4℃. The pellet was resuspended in cytoplasm extraction buffer (10 mM HEPES pH 7.5, 40 mM KCl, 2 mM $MgCl_2$, 10% glycerol, 0.125% NP-40) containing protease inhibitor cocktail (Roche Diagnostics, Mannheim, Germany) and phosphatase inhibitors (Roche Diagnostics). The cytosol fraction was obtained after incubation on ice and centrifugation at 1000 ***g*** for 10 min. The pellet was cleaned by resuspension in 0.35 M and 0.25 M sucrose buffer and centrifugation at 1430 g for 5 min (4℃). Following resuspension in nuclear lysis buffer (10 mM HEPES pH 7.5, 500 mM NaCl, 1% Triton X-100, 10% glycerol), protease and phosphatase inhibitor cocktails were added. The pellet was sonicated (10 s at 30% power) and the nuclear fraction was collected as a supernatant after centrifugation at 22,000 ***g*** for 15 min at 4℃.

Phosphoproteomics

Whole HCT116 cell lysates, from cells that were either treated with 0.66 ng/ml of TNF (Immunotools, Germany) or untreated were maintained for 48 h and incubated for 2 h at 37℃ on phosphopeptide slides. The standard layout contained 1024 peptides in triplicate with 32×32 spots in each replicate subarray (4×4 fields in each replicate subarray with 8×8 spots in each field) (Pepscan, Lelystad, Netherlands). The experiment was performed with two independent treatments in the presence of radioactive [^{33}P]-ATP. After washing, phosphopeptide platforms were analyzed by using GenePixPro6 software.

Plasmids and transfection

The human pRK5F-DAPK-Flag plasmid was a kind gift from Dr Ruey-Hwa Chen (National Taiwan University, Taipei). The human HSF1-HA construct was kindly provided by Dr Yun-Sil Lee (Korea Institute of Radiological and Medical Sciences, Seoul). Site-directed mutagenesis was performed using the PCR extension procedure. All clones were sequenced in their entirety. Transfection of HCT116 cells was performed using Lipofectamine 2000 transfection reagent (Invitrogen) in accordance with the manufacturer's instructions.

RNA isolation and qRT-PCR

The RNAeasy Mini Kit (Qiagen, Hilden, Germany) was used for RNA extraction. Synthesis of cDNA was performed using the QuantiTest RT Kit (Qiagen). Real-time PCR analysis using SYBR Green PCR Master Mix (Qiagen) was performed on a CFX96 Real-time PCR Detection system (Biorad). Primer sequences are available in supplementary material Table S3. For data analysis, raw counts were normalized to the expression of the β-2-macroglobulin gene for the same time point and condition (ΔCt). Fold induction was calculated as described previously (Bajbouj et al., 2009).

siRNA-mediated knockdown

Human HSF1 siRNA (Santa Cruz, sc-35611) was used as pool of three different siRNA duplexes. 35611A sense, 5′-CCCAUCAUCUCCGACA-UCATT-3′; antisense, 5′-UGAUGUCGGAGAUGAUGGGTT-3′; 35611B sense, 5′-GUGACCACUUGGAUGCUAUTT-3′; antisense, 5′-AUAGCA-UCCAAGUGGUCACTT-3′; 35611C sense, 5′-CGUGUCCUGUGGU-UUGGUUTT-3′; antisense, 5′-AACCAAACCACAGGACACGTT-3′. Scrambled siRNA A (Santa Cruz, sc-37007) was used. Cells were transfected using Lipofectamine 2000 (Invitrogen) in accordance with the manufacturer's protocol, followed by a change of medium and exposure to TNF.

Immunofluorescence microscopy

Cells were grown on coverslips and fixed in 3.7% paraformaldehyde, permeabilized and stained with primary antibodies against DAPK (BD Biosciences; 1:250) or pHSF1^{Ser230} (Santa Cruz; 1:100) overnight at 4℃, followed by incubation with secondary anti-mouse-IgG or anti-rabbit-IgG antibodies conjugated to Alexa Fluor 488 or Alexa Fluor 555 (Invitrogen; 1:500) for 2 h at room temperature. Slides were examined and photographed using a confocal laser-scanning microscopy system (LSM T-PMT Observer Z1, Carl Zeiss Inc., Thornwood, NY) with a 63× oil objective. Nuclei were counterstained with 4′,6-diamino-2-phenylindole (DAPI).

Flow cytometry

Annexin-V-Fluous staining was performed in accordance with the manufacturer's protocol (Roche Diagnostics). Flow cytometry analysis was performed on a BD FACS Canto II after gating and excluding cell debris. Data were analyzed using FlowJo software.

Bioinformatic analysis of the DAPK–HSF1 interaction

Information about phosphorylation sites in HSF1 was obtained from the PhosphoSite (http://www.phosphosite.org; Hornbeck et al., 2004) and PhosphoELM (http://phospho.elm.eu.org; Dinkel et al., 2011). Non-globular protein segments were predicted using GlobPlot 2.3 (http://globplot.embl.de) (Linding et al., 2003). NLS sequences were predicted with NLS mapper (http://nls-mapper.iab.keio.ac.jp) (Kosugi et al., 2009). Modeling of DAPK in complex with the HSF1 sequence stretch containing Ser230 was performed using Modeller (Sánchez and Sali, 2000). For DAPK, modeling was based on the nucleotide-bound crystal structure of DAPK (PDB code: 3F5U) (McNamara et al., 2009, Fig. 2A). The geometry of the substrate was adapted from a crystal structure of the homologous phosphorylase kinase peptide substrate complex (PDB code: 2PHK) (Lowe et al., 1997). Structural analysis and visualization were performed using RasMol (Sayle and Milner-White, 1995).

Structural modeling of DAPK–HSF1–CAMKII complex

The structure of the catalytic domain of DAPK (PDB:1JKS – X-ray structure of the catalytic domain of human DAPK at 1.5 Å resolution) was used as a template for modeling DAPK. Human HSF1 was modeled using the following templates to cover the stretch of sequence covering the 529-amino-acid region. The PDB structures considered for modeling were: 2LDU (10–123), 4DZM and 1EXU (126–203), 3K9J (200–260), 2VBC (203–310), 1Z05 (311–371), 2WLX and 3OOQ (371–529). In order to investigate a competitive inhibition between the DAPK and CAMKII, a DAPK–HSF1–CAMKII complex was modeled. The active conformation of the catalytic domain of human CAMKII was modeled using Modeller 9v12 with the structure of CAMKII (PDB ID: 3KK8 – X-ray structure of *Caenorhabditis elegans* CAMKII kinase domain at 1.72 Å resolution) (Chao et al., 2010) as the template.

The catalytic domain of DAPK (PDB: 1JKS) was then docked to modeled HSF1 phosphorylated at Ser230. The catalytic domain of CAMKII was docked to the DAPK–HSFI complex. The docking, energy filtering and ranking of the complexes of these structures were performed by the ClusPro server. In all cases, the top 1000 structures were chosen after energy filtering (electrostatics), clustered and ranked according to cluster sizes. The hydrogen bond interactions in the DAPK–HSF1 complex and the DAPK–CAMKII–HSF1 (Fig. 1C) complex were analyzed using HBOND Calculator (http://cib.cf.ocha.ac.jp/bitool/HBOND/) and are summarized in supplementary material Tables S2 and S3. All renderings were performed using Chimera 1.8 (Pettersen et al., 2004).

Docking of the DAPK inhibitor to the DAPK/HSF1 complex

The DAPK inhibitor was docked to the catalytic domain of DAPK (PDB ID: 1JKS) and to the DAPK–HSF1 complex. The structure of the

inhibitor was drawn previously using PubChem Sketcher V2.4 (Ihlenfeldt et al., 2009) and was further prepared for docking using the LigPrep module of Schrödinger (LigPrep, version 2.5, Schrödinger, LLC, New York, NY, 2012). Protein preparation was performed using the Protein preparation wizard of Schrödinger suite. Flexible docking was performed using the extra precision mode of Glide module (Friesner et al., 2006). Analysis of the conformational changes of DAPK was performed using VMD 1.9.1 and rendering was performed using Chimera 1.8.

Immunoprecipitation-*in vitro* kinase assay

Recombinant DAPK-1 was purchased from Biaffin GmbH (Kassel, Germany). For the immunoprecipitation-kinase assay, cells in 10-cm dishes were transiently transfected with 24 µg of cDNA encoding wild-type and mutant HSF by using Lipofectamine 2000 (Invitrogen) transfection reagent. After performing the immunoprecipitation using the anti-HSF1 antibody (Cell Signaling Technology) on magnetic beads (Invitrogen) containing immobilized substrate, 0.6–1.2 µg of active DAPK-1 was added in the presence of 7.5 µCi [γ-^{32}P]-ATP (Hartmann Analytic, Braunschweig, Germany) and 200 µM cold ATP in the DAPK reaction buffer (Chen et al., 2005) for 30 min at 30°C. For the reverse kinase assay, wild-type DAPK and the K42A, S308A and S308E mutants and empty vector were overexpressed in HCT116 cells during a 24-h exposure to TNF, followed by immunoprecipitation in RIPA buffer using a specific DAPK antibody (BD Biosciences). The next day, beads were washed in washing buffer, activated in kinase buffer and incubated with recombinant HSF1 protein (Novus Biologicals, Cambridge, UK) in the presence of radioactive ATP for 30 min at 30°C. The reaction was stopped by adding SDS-containing lysis buffer. Proteins were then resolved by SDS-PAGE and detected by autoradiography.

For the *in vitro* phosphorylation reaction in the presence of 200 µM cold ATP only, we used 0.6 µg of DAPK–GST recombinant enzyme, 0.8 µg of HSF1–His recombinant protein and 0.8 µg of GST recombinant protein in the DAPK kinase buffer. The incubation was performed at 30°C for 30 min in the absence or presence of 30 µM and 100 µM DAPK inhibitor. The kinase reaction was stopped by adding 5× protein loading buffer and boiling at 95°C for 5 min. The samples were resolved on 7.5% SDS-PAGE and immunoblotted using phospho-specific antibody. For DAPK detection, a specific antibody against DAPK-1 [EPR1818 (2), Abcam, Cambridge, MA] was used.

In vitro binding assay

First, GST protein (Novus Biologicals, Littleton, CO) or GST-tagged DAPK recombinant protein (Biaffin, Kassel, Germany) (0.5 µg/ml) was immobilized on glutathione–agarose beads (Sigma-Aldrich) by incubation in binding buffer (1×PBS, 0.1% NP40, 0.5 mM DTT, 10% glycerol, 1 mM PMSF, 2 µg/ml aprotinin) for 2 h at 4°C. Beads were washed three times in the binding buffer. Equal amounts of HSF1–His recombinant protein were added to the GST- or DAPK-beads, and the samples were incubated in 200 µl of binding buffer overnight at 4°C. After washing three times in PBS, protein loading buffer was added to the beads and boiled at 95°C for 5 min. The eluent was analyzed by western blotting using specific antibodies. For DAPK detection, a specific antibody against DAPK-1 [EPR1818 (2), Abcam] was used.

Luciferase reporter assay

The dual GLuc/SeAP promoter reporter clone for human DAPK1 (NM_004938) (HRPMI16618-PG04) contains a 1.4 kb insert corresponding to the 5′-flanking promoter sequence located 1393 bp upsteam and 47 bp downstream of the transcription start site of a human DAPK gene. The negative control clone NEG-PG04 and the positive control clone GAPDH-PG04 were obtained from GeneCopoeia. The parallel bioluminescence assay of *Gaussia* luciferase (GLuc) and secreted alkaline phosphatase (SeAP) was performed by using the Secrete-Pair™ Dual Luminescence assay kit (GeneCopoeia, Rockville, MD) in accordance with the manufacturer's protocol. Signal normalization was performed using SeAP signal as an internal standard control (GLuc/SeAP) in order to eliminate the impact of transfection efficiency variations among the cell samples. All luciferase results are reported as relative light units (RLU). Luciferase experiments were performed in triplicate and repeated three times independently. The data presented are representative experiments.

Chromatin immunoprecipitation

ChIP assays were performed in accordance with the manufacturer's instructions (ChIP-IT™ Express Kit; Active Motif, Carlsbad, CA). The purified DNA was subjected to real-time PCR amplification for the heat shock response element (HSE) within the human DAPK promoter using site-specific primers: sense, 5′-ATGAGGTACGCTCCCTTCCT-3′ and antisense, 5′-TCGTCCCGAGATGTGTACTG-3′. The sequence of the control F2/R2 and F3/R3 oligonucleotides is given in supplementary material Table S4. The product was quantified using a real-time PCR system (Biorad). Reactions were performed in triplicate, and the mean was normalized to input chromatin and reported as relative fold enrichment (±s.d.). All ChIP assays were repeated at least three times.

Human samples and immunohistochemical analysis

All experiments performed were approved by the local ethics committee. Paraffin-embedded tissue samples were obtained from the Institute of Pathology, Friedrich-Alexander-University Erlangen-Nürnberg, Germany. TMA was generated from patient material. A 5-µm thick section was cut from each paraffin block and the histological mirror image on a hematoxylin and eosin slice was evaluated by expert pathologists (T.T.R., A.A. and S.S.). The group of colorectal patients (n=53) was 52.8% male and 47.2% female. The age at which patients were diagnosed with a tumor ranged from 35 to 91, with a mean age of 69 years in the female subgroup and 70 years in the male subgroup. The clinical data of the patients is presented in supplementary material Table S5.

Immunohistochemistry was performed as described previously (Chakilam et al., 2013). Tissue sections were counterstained with hematoxylin (Merck KGaA, Darmstadt, Germany) and specific antibodies – rabbit polyclonal anti-pHSF1^{Ser230} (Santa Cruz; 1:20) and mouse monoclonal anti-DAPK (BD Biosciences; 1:250). All sections were counterstained with Mayer's Hemalaun solution (Merck). Appropriate negative controls were included (supplementary material Fig. S3A,B). The staining intensity of immunopositive cells was visually scored semi-quantitatively as the percentage of positive cells with intensity scores of 0–3, according to the Remmele score (Remmele and Stegner, 1987).

Statistical analysis

Results are expressed as the mean±s.d. or ±s.e.m. We utilized unpaired Student's t-tests for all pair-wise comparisons. P-values of <0.05 were considered as significant. For human tissue microarray analysis, SPSS software (v.19.0.0) was used.

Acknowledgements

We thank Ruey-Hwa Chen for providing the DAPK-FLAG construct as well as Yun-Sil Lee for providing HSF1–HA and pHACE–HA expression plasmids. We thank Olaf Prante for help in performing the radioisotope experiments. We would like to thank Adrian Koch for his excellent technical assistance with FACS analysis, Rudolph Jung and Christa Winkelmann for the assistance with immunohistochemistry experiments and Maria Leidenberger for technical help in immunoblotting.

Competing interests

The authors declare no competing interests.

Author contributions

N.B. carried out most of the experiments. J.I. performed cellular fractionation and immunoblotting experiments. T.T.R., A.A. and S.S. analyzed the tissue microarrays. J.S.-L. generated HSF1 mutants. S.C. and M.G. performed immunoblotting experiments. E.Z. and T.F. performed and analyzed phosphopeptide arrays. S.M. performed bioinformatical modeling. V.M. and H.S. generated in silico models, analyzed bioinformatical data and wrote the manuscript chapter. L.D. designed irradiation tissue microarrays. R.S.-S. and N.B. designed experiments, analyzed data and wrote the manuscript. All authors read and approved the final manuscript.

Funding

This work was supported by research grants from the Deutsche Forschungsgemeinschaft [grant number SCHN477-9-2 to R.S.-S.];

Manfred-Stolte Stiftung [grant numbers 38736003, 38736005, 38736007 to R.S.-S.]; Interdisciplinary Centre for Clinical Research [grant number IZKF-D18 to R.S.-S.]; and Deutsche Krebshilfe [grant number 107153 (TP3) to T.F.].

Supplementary material

Supplementary material available online at
http://jcs.biologists.org/lookup/suppl/doi:10.1242/jcs.157024/-/DC1

References

Bajbouj, K., Poehlmann, A., Kuester, D., Drewes, T., Haase, K., Hartig, R., Teller, A., Kliche, S., Walluscheck, D., Ivanovska, J. et al. (2009). Identification of phosphorylated p38 as a novel DAPK-interacting partner during TNFalpha-induced apoptosis in colorectal tumor cells. *Am. J. Pathol.* **175**, 557-570.

Benderska, N. and Schneider-Stock, R. (2014). Transcription control of DAPK. *Apoptosis* **19**, 298-305.

Benderska, N., Chakilam, S., Hugle, M., Ivanovska, J., Gandesiri, M., Schulze-Luhrmann, J., Bajbouj, K., Croner, R. and Schneider-Stock, R. (2012). Apoptosis signalling activated by TNF in the lower gastrointestinal tract. Review. *Curr. Pharm. Biotechnol.* **13**, 2248-2258.

Bialik, S. and Kimchi, A. (2006). The death-associated protein kinases: structure, function, and beyond. *Annu. Rev. Biochem.* **75**, 189-210.

Bialik, S. and Kimchi, A. (2012). Biochemical and functional characterization of the ROC domain of DAPK establishes a new paradigm of GTP regulation in ROCO proteins. *Biochem. Soc. Trans.* **40**, 1052-1057.

Bialik, S., Berissi, H. and Kimchi, A. (2008). A high throughput proteomics screen identifies novel substrates of death-associated protein kinase. *Mol. Cell. Proteomics* **7**, 1089-1098.

Bovellan, M., Fritzsche, M., Stevens, C. and Charras, G. (2010). Death-associated protein kinase (DAPK) and signal transduction: blebbing in programmed cell death. *FEBS J.* **277**, 58-65.

Calderwood, S. K., Xie, Y., Wang, X., Khaleque, M. A., Chou, S. D., Murshid, A., Prince, T. and Zhang, Y. (2010). Signal transduction pathways leading to heat shock transcription. *Sign Transduct Insights* **2**, 13-24.

Castro, F., Dirks, W. G., Fähnrich, S., Hotz-Wagenblatt, A., Pawlita, M. and Schmitt, M. (2013). High-throughput SNP-based authentication of human cell lines. *Int. J. Cancer* **132**, 308-314.

Chakilam, S., Gandesiri, M., Rau, T. T., Agaimy, A., Vijayalakshmi, M., Ivanovska, J., Wirtz, R. M., Schulze-Luehrmann, J., Benderska, N., Wittkopf, N. et al. (2013). Death-associated protein kinase controls STAT3 activity in intestinal epithelial cells. *Am. J. Pathol.* **182**, 1005-1020.

Chao, L. H., Pellicena, P., Deindl, S., Barclay, L. A., Schulman, H. and Kuriyan, J. (2010). Intersubunit capture of regulatory segments is a component of cooperative CaMKII activation. *Nat. Struct. Mol. Biol.* **17**, 264-272.

Chen, C. H., Wang, W. J., Kuo, J. C., Tsai, H. C., Lin, J. R., Chang, Z. F. and Chen, R. H. (2005). Bidirectional signals transduced by DAPK-ERK interaction promote the apoptotic effect of DAPK. *EMBO J.* **24**, 294-304.

Chen, H. Y., Lee, Y. R. and Chen, R. H. (2014). The functions and regulations of DAPK in cancer metastasis. *Apoptosis* **19**, 364-370.

Chu, B., Soncin, F., Price, B. D., Stevenson, M. A. and Calderwood, S. K. (1996). Sequential phosphorylation by mitogen-activated protein kinase and glycogen synthase kinase 3 represses transcriptional activation by heat shock factor-1. *J. Biol. Chem.* **271**, 30847-30857.

Cohen, O., Inbal, B., Kissil, J. L., Raveh, T., Berissi, H., Spivak-Kroizaman, T., Feinstein, E. and Kimchi, A. (1999). DAP-kinase participates in TNF-alpha- and Fas-induced apoptosis and its function requires the death domain. *J. Cell Biol.* **146**, 141-148.

Deiss, L. P., Feinstein, E., Berissi, H., Cohen, O. and Kimchi, A. (1995). Identification of a novel serine/threonine kinase and a novel 15-kD protein as potential mediators of the gamma interferon-induced cell death. *Genes Dev.* **9**, 15-30.

Dinkel, H., Chica, C., Via, A., Gould, C. M., Jensen, L. J., Gibson, T. J. and Diella, F. (2011). Phospho.ELM: a database of phosphorylation sites – update 2011. *Nucleic Acids Res.* **39**, D261-D267.

Edmondson, D. G., Davie, J. K., Zhou, J., Mirnikjoo, B., Tatchell, K. and Dent, S. Y. (2002). Site-specific loss of acetylation upon phosphorylation of histone H3. *J. Biol. Chem.* **277**, 29496-29502.

Eisenberg-Lerner, A. and Kimchi, A. (2007). DAP kinase regulates JNK signaling by binding and activating protein kinase D under oxidative stress. *Cell Death Differ.* **14**, 1908-1915.

Friesner, R. A., Murphy, R. B., Repasky, M. P., Frye, L. L., Greenwood, J. R., Halgren, T. A., Sanschagrin, P. C. and Mainz, D. T. (2006). Extra precision glide: docking and scoring incorporating a model of hydrophobic enclosure for protein-ligand complexes. *J. Med. Chem.* **49**, 6177-6196.

Gandesiri, M., Chakilam, S., Ivanovska, J., Benderska, N., Ocker, M., Di Fazio, P., Feoktistova, M., Gali-Muhtasib, H., Rave-Fränk, M., Prante, O. et al. (2012). DAPK plays an important role in panobinostat-induced autophagy and commits cells to apoptosis under autophagy deficient conditions. *Apoptosis* **17**, 1300-1315.

Holmberg, C. I., Hietakangas, V., Mikhailov, A., Rantanen, J. O., Kallio, M., Meinander, A., Hellman, J., Morrice, N., MacKintosh, C., Morimoto, R. I. et al. (2001). Phosphorylation of serine 230 promotes inducible transcriptional activity of heat shock factor 1. *EMBO J.* **20**, 3800-3810.

Holtmann, H., Hahn, T. and Wallach, D. (1988). Interrelated effects of tumor necrosis factor and interleukin 1 on cell viability. *Immunobiology* **177**, 7-22.

Hornbeck, P. V., Chabra, I., Kornhauser, J. M., Skrzypek, E. and Zhang, B. (2004). PhosphoSite: A bioinformatics resource dedicated to physiological protein phosphorylation. *Proteomics* **4**, 1551-1561.

Ihlenfeldt, W. D., Bolton, E. E. and Bryant, S. H. (2009). The PubChem chemical structure sketcher. *J. Cheminform* **1**, 20.

Ivanovska, J., Tregubova, A., Mahadevan, V., Chakilam, S., Gandesiri, M., Benderska, N., Ettle, B., Hartmann, A., Söder, S., Ziesché, E. et al. (2013). Identification of DAPK as a scaffold protein for the LIMK/cofilin complex in TNF-induced apoptosis. *Int. J. Biochem. Cell Biol.* **45**, 1720-1729.

Jacobs, A. T. and Marnett, L. J. (2009). HSF1-mediated BAG3 expression attenuates apoptosis in 4-hydroxynonenal-treated colon cancer cells via stabilization of anti-apoptotic Bcl-2 proteins. *J. Biol. Chem.* **284**, 9176-9183.

Jang, C. W., Chen, C. H., Chen, C. C., Chen, J. Y., Su, Y. H. and Chen, R. H. (2002). TGF-beta induces apoptosis through Smad-mediated expression of DAP-kinase. *Nat. Cell Biol.* **4**, 51-58.

Jin, Y. and Gallagher, P. J. (2003). Antisense depletion of death-associated protein kinase promotes apoptosis. *J. Biol. Chem.* **278**, 51587-51593.

Jin, Y., Blue, E. K. and Gallagher, P. J. (2006). Control of death-associated protein kinase (DAPK) activity by phosphorylation and proteasomal degradation. *J. Biol. Chem.* **281**, 39033-39040.

Kissil, J. L., Feinstein, E., Cohen, O., Jones, P. A., Tsai, Y. C., Knowles, M. A., Eydmann, M. E. and Kimchi, A. (1997). DAP-kinase loss of expression in various carcinoma and B-cell lymphoma cell lines: possible implications for role as tumor suppressor gene. *Oncogene* **15**, 403-407.

Kosugi, S., Hasebe, M., Tomita, M. and Yanagawa, H. (2009). Systematic identification of cell cycle-dependent yeast nucleocytoplasmic shuttling proteins by prediction of composite motifs. *Proc. Natl. Acad. Sci. USA* **106**, 10171-10176.

Kuo, J. C., Lin, J. R., Staddon, J. M., Hosoya, H. and Chen, R. H. (2003). Uncoordinated regulation of stress fibers and focal adhesions by DAP kinase. *J. Cell Sci.* **116**, 4777-4790.

Leung, R. C., Liu, S. S., Chan, K. Y., Tam, K. F., Chan, K. L., Wong, L. C. and Ngan, H. Y. (2008). Promoter methylation of death-associated protein kinase and its role in irradiation response in cervical cancer. *Oncol. Rep.* **19**, 1339-1345.

Linding, R., Russell, R. B., Neduva, V. and Gibson, T. J. (2003). GlobPlot: Exploring protein sequences for globularity and disorder. *Nucleic Acids Res.* **31**, 3701-3708.

Lowe, E. D., Noble, M. E., Skamnaki, V. T., Oikonomakos, N. G., Owen, D. J. and Johnson, L. N. (1997). The crystal structure of a phosphorylase kinase peptide substrate complex: kinase substrate recognition. *EMBO J.* **16**, 6646-6658.

McMillan, D. R., Xiao, X., Shao, L., Graves, K. and Benjamin, I. J. (1998). Targeted disruption of heat shock transcription factor 1 abolishes thermotolerance and protection against heat-inducible apoptosis. *J. Biol. Chem.* **273**, 7523-7528.

McNamara, L. K., Watterson, D. M. and Brunzelle, J. S. (2009). Structural insight into nucleotide recognition by human death-associated protein kinase. *Acta Crystallogr. D Biol. Crystallogr.* **65**, 241-248.

Mendillo, M. L., Santagata, S., Koeva, M., Bell, G. W., Hu, R., Tamimi, R. M., Fraenkel, E., Ince, T. A., Whitesell, L. and Lindquist, S. (2012). HSF1 drives a transcriptional program distinct from heat shock to support highly malignant human cancers. *Cell* **150**, 549-562.

Michie, A. M., McCaig, A. M., Nakagawa, R. and Vukovic, M. (2010). Death-associated protein kinase (DAPK) and signal transduction: regulation in cancer. *FEBS J.* **277**, 74-80.

Min, J. N., Huang, L., Zimonjic, D. B., Moskophidis, D. and Mivechi, N. F. (2007). Selective suppression of lymphomas by functional loss of Hsf1 in a p53-deficient mouse model for spontaneous tumors. *Oncogene* **26**, 5086-5097.

Mittag, F., Kuester, D., Vieth, M., Peters, B., Stolte, B., Roessner, A. and Schneider-Stock, R. (2006). DAPK promotor methylation is an early event in colorectal carcinogenesis. *Cancer Lett.* **240**, 69-75.

Morimoto, R. I. (1998). Regulation of the heat shock transcriptional response: cross talk between a family of heat shock factors, molecular chaperones, and negative regulators. *Genes Dev.* **12**, 3788-3796.

Morimoto, R. I., Kroeger, P. E. and Cotto, J. J. (1996). The transcriptional regulation of heat shock genes: a plethora of heat shock factors and regulatory conditions. *EXS* **77**, 139-163.

Murshid, A., Chou, S. D., Prince, T., Zhang, Y., Bharti, A. and Calderwood, S. K. (2010). Protein kinase A binds and activates heat shock factor 1. *PLoS ONE* **5**, e13830.

Nakai, A., Suzuki, M. and Tanabe, M. (2000). Arrest of spermatogenesis in mice expressing an active heat shock transcription factor 1. *EMBO J.* **19**, 1545-1554.

Pettersen, E. F., Goddard, T. D., Huang, C. C., Couch, G. S., Greenblatt, D. M., Meng, E. C. and Ferrin, T. E. (2004). UCSF chimera – a visualization system for exploratory research and analysis. *J. Comput. Chem.* **25**, 1605-1612.

Pike, A. C., Rellos, P., Niesen, F. H., Turnbull, A., Oliver, A. W., Parker, S. A., Turk, B. E., Pearl, L. H. and Knapp, S. (2008). Activation segment dimerization: a mechanism for kinase autophosphorylation of non-consensus sites. *EMBO J.* **27**, 704-714.

Raval, A., Tanner, S. M., Byrd, J. C., Angerman, E. B., Perko, J. D., Chen, S. S., Hackanson, B., Grever, M. R., Lucas, D. M., Matkovic, J. J. et al. (2007). Downregulation of death-associated protein kinase 1 (DAPK1) in chronic lymphocytic leukemia. *Cell* **129**, 879-890.

Raveh, T. and Kimchi, A. (2001). DAP kinase-a proapoptotic gene that functions as a tumor suppressor. *Exp. Cell Res.* **264**, 185-192.
Raveh, T., Droguett, G., Horwitz, M. S., DePinho, R. A. and Kimchi, A. (2001). DAP kinase activates a p19ARF/p53-mediated apoptotic checkpoint to suppress oncogenic transformation. *Nat. Cell Biol.* **3**, 1-7.
Remmele, W. and Stegner, H. E. (1987). [Recommendation for uniform definition of an immunoreactive score (IRS) for immunohistochemical estrogen receptor detection (ER-ICA) in breast cancer tissue]. *Pathologe* **8**, 138-140.
Rennier, K. and Ji, J. Y. (2012). Shear stress regulates expression of death-associated protein kinase in suppressing TNFα-induced endothelial apoptosis. *J. Cell. Physiol.* **227**, 2398-2411.
Sánchez, R. and Sali, A. (2000). Comparative protein structure modeling. Introduction and practical examples with modeller. *Methods Mol. Biol.* **143**, 97-129.
Sayle, R. A. and Milner-White, E. J. (1995). RASMOL: biomolecular graphics for all. *Trends Biochem. Sci.* **20**, 374.
Schneider-Stock, R. (2014). Death-associated kinase (DAPK): a cancer ''gene chameleon''. *Apoptosis* **19**, 285.
Temmerman, K., Simon, B. and Wilmanns, M. (2013). Structural and functional diversity in the activity and regulation of DAPK-related protein kinases. *FEBS J.* **280**, 5533-5550.
Tran, S. E., Meinander, A., Holmström, T. H., Rivero-Müller, A., Heiskanen, K. M., Linnau, E. K., Courtney, M. J., Mosser, D. D., Sistonen, L. and Eriksson, J. E. (2003). Heat stress downregulates FLIP and sensitizes cells to Fas receptor-mediated apoptosis. *Cell Death Differ.* **10**, 1137-1147.
Trinklein, N. D., Murray, J. I., Hartman, S. J., Botstein, D. and Myers, R. M. (2004). The role of heat shock transcription factor 1 in the genome-wide regulation of the mammalian heat shock response. *Mol. Biol. Cell* **15**, 1254-1261.
Wang, X., Khaleque, M. A., Zhao, M. J., Zhong, R., Gaestel, M. and Calderwood, S. K. (2006). Phosphorylation of HSF1 by MAPK-activated protein kinase 2 on serine 121, inhibits transcriptional activity and promotes HSP90 binding. *J. Biol. Chem.* **281**, 782-791.
Wu, C. (1995). Heat shock transcription factors: structure and regulation. *Annu. Rev. Cell Dev. Biol.* **11**, 441-469.
Xia, W., Voellmy, R. and Spector, N. L. (2000). Sensitization of tumor cells to fas killing through overexpression of heat-shock transcription factor 1. *J. Cell. Physiol.* **183**, 425-431.
Zalckvar, E., Berissi, H., Eisenstein, M. and Kimchi, A. (2009). Phosphorylation of Beclin 1 by DAP-kinase promotes autophagy by weakening its interactions with Bcl-2 and Bcl-XL. *Autophagy* **5**, 720-722.